# Magnesium stable isotopes as a potential geochemical tool in agronomy – Constraints and opportunities

David Uhlig<sup>1\*</sup>, Bei Wu<sup>1</sup>, Anne E. Berns<sup>1</sup>, Wulf Amelung<sup>1,2</sup>

### **Abstract**

A sustainable use of soil resources is urgently required to cope with the increasing demand for agricultural products during climate change. To inspire farmers on new soil cultivation methods like subsoil management requires not only yield measurements but also nutrient use efficiency measurements for which analytical tools are still missing. Stable isotopes of the macronutrient magnesium (Mg) are a potential novel subsoil management evaluation tool in agronomy and soil/plant sciences because its isotope ratios shift considerably during Mg uptake by crops. The feasibility of Mg stable isotopes was first demonstrated conceptually by simulating subsoil management on soils with low, middle, and high inventories of bioavailable Mg and crop plants typically cultivated in Germany. This simulation showed that the magnitude of Mg isotope shifts among crops and the exchangeable fraction of Mg in soil is resolvable from the long-term external precision of Mg isotope analyses only if three conditions are met. First, the crop uptake-related Mg isotope fractionation factor should be at the upper end of hitherto published fractionation factors. Second, a high Mg uptake flux of crop plants (e.g., sugar beets) is matched by a low Mg supply from the exchangeable fraction in soil (e.g., sandy soils). Third, subsoil management causes a considerable deepening of the rooting system (e.g., flipping the topsoil root cluster below 30 cm depth). If these conditions are met, Mg stable isotopes can be used in a qualitative manner to identify the main Mg uptake depth, and in a quantitative manner by calculating the Mg use efficiency, defined here as the ratio of Mg uptake versus Mg supply, solely from Mg isotope ratios. This concept was tested for Alfisols on field trials by conducting deep loosening with and without the incorporation of compost. Magnesium isotope shifts in crops and the exchangeable fraction of Mg in soil were mostly unresolvable from the long-term external precision of Mg isotope analyses, which positively tested the Mg isotope concept for well nurtured soils. However, systematic Mg isotope shifts among bulk crops cultivated on and beside a melioration strip were found and attributed to the uplift of isotopically distinct compost-derived Mg on the melioration strip and root restricting layers beside the melioration strip. Given that the Mg isotope composition of the exchangeable fraction barely varies with depth, field-based crop uptake-related 'apparent' Mg isotope

<sup>&</sup>lt;sup>1</sup> Institute of Bio- and Geosciences (IBG-3) Agrosphere, Forschungszentrum Jülich GmbH, Wilhelm-Johnen Straße, 52425 Jülich, Germany

<sup>\*</sup> Corresponding author: d.uhlig@fz-juelich.de

<sup>&</sup>lt;sup>2</sup> Institute of Crop Science and Resource Conservation – Soil Science and Soil Ecology, University of Bonn, Nussallee 13, 53115 Bonn, Germany

fractionation factors of winter wheat and spring barley could be determined, which differed from one another ( $\Delta^{26}$ Mg<sub>wheat-rem.exch.</sub> = 0.63 ± 0.05‰,  $\Delta^{26}$ Mg<sub>barley-rem.exch.</sub> = 0.37 ± 0.12‰). Nonetheless, the quantitative approach of Mg isotopes was violated when calcareous fertilizer was applied to the field as differences in the isotope-derived Mg use efficiency could be attributed to the uneven distribution of lime-derived Mg with depth. Using Mg stable isotopes as a new geochemical routine for agronomy and soil/plant sciences requires future work focussing on isotope fractionation factors related to crop uptake and intra-plant translocation of Mg – which may depend on species, environmental conditions, and nutrient status – to allow minimally invasive sampling of the soil-plant system and to reduce sample sets.

Keywords: Conceptual isotope model | Mg isotopes | fractionation factor | subsoil management| agricultural lime

#### **Highlights**

- 1. A conceptual Mg isotope model was established and positively tested in the field.
- 2. Mg stable isotopes are a powerful novel tool for subsoil management evaluation.
- 3. Mg use efficiency of crops can solely be quantified from Mg stable isotopes.
- 4. Lime application limits Mg use efficiency determination solely from Mg isotopes.
- 5. A criteria catalogue ensures a successful application of Mg isotopes in agronomy.

#### 1. Introduction

The ongoing growth of the global population has dramatically increased human demand for agricultural products. As a result, land use changes, land use intensification and yield improvements boosted cereal production by about 240% from 1961-2017 (IPCC, 2019) but also caused negative effects on the environment. To avoid further conversions of natural ecosystems to intensely managed agricultural land, and to cope with more frequent summer droughts caused by climate change, an efficient use of soil resources is urgently required.

Traditionally, the productivity of agricultural land was almost exclusively maintained in the plough horizon, the agricultural topsoil. However, the subsoil beneath this tilled layer contains an inherent large reservoir of bioavailable mineral nutrients and water (Kautz et al., 2013; Kirkegaard et al., 2007). In principle, these resources are accessible to crops as evidenced by the crop's global mean maximum rooting depth of 200 cm (Canadell et al., 1996). About 30% of crop root biomass is globally located at 30-200 cm depth (Jackson et al., 1996). However, many soils have root restricting layers in the upper meter of soil, which affect, for example, up to 71% of Germanys agricultural soils (Schneider

and Don, 2019a). Effective means to reduce the penetration resistance for crops include physical melioration, e.g., deep loosening, and biological melioration, e.g., generation of biopores by deep rooting pre-crops (Schneider and Don, 2019b). These melioration strategies do not only enhance root growth into the subsoil (Jakobs et al., 2019) but also increase water infiltration (Blanco-Canqui et al., 2017), which promotes crop yield, especially in dry years (Gaiser et al., 2012; Marks and Soane, 1987; Olesen and Munkholm, 2007). Deep loosening combined with the incorporation of organic matter also optimizes soil pH, increases nitrogen availability (Odlare et al., 2008), and thus improves grain yield (Jakobs et al., 2019). Whereas changes in crop yield can easily be proved, there is still a lack of analytical tools to detect changes of the nutrient uptake depth and/or nutrient use efficiency.

A potential analytical tool for the determination of the nutrient uptake depth is a conservative isotope proxy, such as the radiogenic strontium isotope ratio <sup>87</sup>Sr/<sup>86</sup>Sr, which is insensitive to isotope shifts during soil-plant processes. Therefore, the <sup>87</sup>Sr/<sup>86</sup>Sr ratio of individual plant organs serves as a fingerprint of the <sup>87</sup>Sr/<sup>86</sup>Sr ratio of the Sr source at depth (e.g., Bélanger and Holmden, 2010; Coble et al., 2015; McCulley et al., 2004; Uhlig et al., 2020). Yet, the radiogenic Sr isotope proxy reaches its limitations when a depth gradient in <sup>87</sup>Sr/<sup>86</sup>Sr of the plant's Sr source is lacking. Fortunately, metal(loid) stable isotope ratios of nutrient elements that are strongly cycled in the soil-plant systems provide an alternative isotope proxy that does not require a depth gradient in the isotope composition of the crop's nutrient source.

The stable isotopes of magnesium (<sup>24</sup>Mg, <sup>25</sup>Mg, <sup>26</sup>Mg) – a macronutrient for higher plants (Marschner, 2011) and a major constituent of the bulk silicate Earth – have such a large relative mass difference that the isotope ratio  $^{26}$ Mg/ $^{24}$ Mg, reported as  $\delta^{26}$ Mg value, varies by up to 7‰ in terrestrial material formed by low-temperature (bio)geochemical processes (Young and Galy (2004), Schmitt et al., (2012), Bullen (2014), Teng (2017)). One of the two main processes fractionating Mg isotopes in the soil-plant system is the neoformation of Mg-bearing secondary solids (Mg-clays, Mg-carbonates) as demonstrated for Mg-clays in laboratory experiments (Hindshaw et al., 2020; Li et al., 2021; Ryu et al., 2016; Wimpenny et al., 2014), and under natural conditions in the field (Gao et al., 2018; Liu et al., 2014; Opfergelt et al., 2012; Teng et al., 2010b; Tipper et al., 2010, 2012). The sense of Mg isotope fractionation during neoformation of Mg-clays depends on the Mg-O bonding length (Hindshaw et al., 2020) and favours either isotopically heavy Mg (e.g., Pogge von Strandmann et al., 2008; Ma et al., 2015; Gao et al., 2018) or light Mg isotopes (e.g., Wimpenny et al., 2010; Li et al., 2014; Hindshaw et al., 2020). The formation of Mg-carbonates favours light Mg isotopes (e.g., Wombacher et al., 2011; Pearce et al., 2012; Mavromatis et al., 2013; Saenger and Wang 2014; Schott et al., 2016; Oelkers et al., 2018). Another main process fractionating Mg isotopes in the soil-plant system is Mg uptake by higher plants and microbes, which favours heavy Mg isotopes as shown experimentally (Black et al., 2008; Bolou-Bi et al., 2010; Fahad et al., 2016; Kimmig et al., 2018; Pokharel et al., 2018, 2017; Wang et al., 2020; Wrobel et al., 2020) and in field studies (Bolou-Bi et al., 2016, 2012; Gao et al., 2018; Mavromatis et al., 2014; Novak et al., 2020b, 2020a; Opfergelt et al., 2014; Schuessler et al., 2018; Tipper et al., 2010; Uhlig et al., 2017; Wang et al., 2021). However, intra-plant translocation from below- to aboveground organs generally favours light Mg isotopes (e.g., Bolou-Bi et al., 2012; Uhlig et al., 2017; Gao et al., 2018; Novak et al., 2020a, b; Wang et al., 2021). In leaves, the synthesis of chlorophyll favours either light Mg isotopes (Black et al., 2008, 2006; Ra et al., 2010) or heavy Mg isotopes (Ra and Kitagawa, 2007), depending on the type of chlorophyll formed (Moynier and Fujii, 2017a). In summary, the sensitivity of Mg to isotope fractionation in the soil-plant system suggests Mg isotopes as a promising, novel, but hitherto underexplored analytical tool to trace and quantify biogeochemical processes in agronomy and soil/plant sciences.

The objective of this study was to use Mg stable isotopes as a proxy for the evaluation of subsoil management methods with respect to the uptake depth and use efficiency of Mg by crops. First, a conceptual framework was introduced to show how Mg stable isotopes could be applied to estimate the magnitude of potential Mg isotope shifts in crop plants and in the bioavailable fraction when simulating subsoil management for a variety of soils with low, medium, and high inventories of bioavailable Mg. Second, this concept was tested by means of field trials on Alfisols. Finally, a criteria catalogue was provided to ensure a successful application of Mg isotopes as a new evaluation tool to assess changes in the crop's Mg uptake depth and/or Mg use efficiency caused by subsoil management.

#### 2. Conceptual framework

A simplified schematic representation of Mg compartments and fluxes in the agricultural soil-plant system is illustrated in Figure 1 as an example for cereal crops. A key feature of the agricultural system is the anthropogenic character of Mg influxes (e.g., fertilisation) and outfluxes (e.g., crop harvest). Another special aspect of the agricultural system deals with recycling of organic-bound Mg in the 'organic nutrient cycle' (Uhlig and von Blanckenburg, 2019). Unlike natural ecosystems comprising perennial plants, where recycled Mg originates mainly from annual aboveground litterfall, in agricultural systems recycled Mg stems mainly from dead roots and any other harvest residues that are returned into topsoil after crop harvest.

Put simply, the soil compartment actively participating in Mg uptake by crops is the bioavailable fraction of Mg. This bioavailable Mg results from the solubilisation of soil constituents (e.g., minerals, soil organic matter (SOM), organic and inorganic fertilizer, agricultural lime) and exchanges with hydrated Mg being electrostatically bound to the negatively charged outer-sphere surfaces of primary phyllosilicates, neoformed secondary solids (e.g., clay minerals, oxides, and hydrated oxides) or organic matter (OM). Thus, the exchangeable fraction of Mg in soil represents Mg

in soil solution, which is bioavailable. A glossary of metrics used throughout this paper is provided in Table 1.

#### 2.1. Magnesium inventories

Terrestrial ecosystems buffer influxes and outfluxes of Mg by storage and recycling (Spohn et al., 2021). The total amount of Mg contained in each soil-plant compartment is represented by the Mg inventory ( $I^{Mg}$ ). The inventory of Mg in bulk crops at any point in time t ( $I^{Mg}_{crop,t}$ ) can be calculated from equation 1, where [Mg] and m are the Mg concentration and dry biomass of individual below- and aboveground organs i, respectively, taken from a standardized area A.

$$I_{crop,t}^{Mg} = \sum_{i=organ}^{i} \frac{[Mg]_i \cdot m_i}{A}$$
 equation 1

The inventory of Mg in the exchangeable fraction in soil being available for crop uptake ( $I_{\rm initial\ exch.}^{\rm Mg}$ ) can be calculated from equation 2, where  $[{\rm Mg}]_{\rm initial\ exch.}$ ,  $\rho$ , and z are the Mg concentration of the exchangeable fraction, the bulk density of soil, and the thickness of soil horizon i, respectively.

$$I_{initial \, exch.}^{Mg} = \sum_{i=0}^{i} [Mg]_{initial \, exch._{i}} \cdot \rho_{i} \cdot z_{i}$$
 equation 2

#### 2.2. Magnesium fluxes

Inventories of soil-plant compartments are linked by fluxes. The main soil-plant Mg flux is represented by the net Mg uptake flux of crops ( $U_{\rm net}^{\rm Mg}$ ) that transfers Mg from the exchangeable fraction into crops.  $U_{\rm net}^{\rm Mg}$  describes the time-integrated change of the crop's Mg inventory from germination ( $t_0$ ) to maturity stage ( $t_m$ ), hence over one annual growing season. Whereas  $U_{\rm net}^{\rm Mg}$  accounts for root mortality, which returns Mg from crops back into soil during ripening, the initial Mg content of the seed can be considered infinitesimal compared with the Mg inventory of the crop at maturity stage.

The inventory of exchangeable Mg is further linked to other compartments by various fluxes. For example, external influxes of Mg include atmospheric wet deposition ( $Dep_{wet}^{Mg}$ ), dry deposition ( $Dep_{dry}^{Mg}$ ), and the application of organic and inorganic fertilizer ( $Dep_{fertilizer}^{Mg}$ ) and agricultural lime ( $Dep_{lime}^{Mg}$ ). Upon solubilisation ( $S_{dry}^{Mg}$ ,  $S_{fertilizer}^{Mg}$ ,  $S_{lime}^{Mg}$ ) these external inputs can impact exchangeable Mg. On the other hand, internal Mg fluxes affecting exchangeable Mg comprise i) the solubilisation of SOM originating mainly from harvest residues returned into topsoil after harvest, dead roots and

microbial necromass  $(S_{SOM}^{Mg})$ , ii) chemical weathering  $(W_{soil}^{Mg})$  that liberates Mg slowly but steadily from soil minerals and amorphous soil constituents, iii) neoformation of secondary solids  $(P_{secondary}^{Mg})$  such as Mg-clays and pedogenic Mg-carbonates that iv) may also be resolubilised  $(S_{secondary}^{Mg})$ . Magnesium outfluxes are, apart from nutrient removal by crop harvest, soil erosion  $(E_{soil}^{Mg})$  and leaching losses  $(W_{leach}^{Mg})$ .

#### 2.3. Magnesium isotopes in the agricultural soil-plant system

From an isotope geochemical point of view the agricultural soil-plant system can be considered as a batch reactor whose compartments interact with one another upon crop harvest, violating Rayleigh effects (e.g., isolation of the growing crop from its Mg source during growth). In this batch reactor Mg isotopes are incompletely partitioned from a source compartment into target compartments that differ in their Mg isotope compositions ( $\delta^{26}$ Mg values) from the source ( $\Delta^{26}$ Mg<sub>target-source</sub>  $\neq$  0%, Figure 2a,d) if the source is not exhausted. The source compartment (Mginitial exch.) is defined as the exchangeable fraction in soil, which rapidly interacts with soil solution from which crops take up Mg. The target compartments comprise crops (Mg<sub>crop</sub>) and the exchangeable fraction that remains in soil after Mg uptake by crops (Mgrem. exch.). Thus, the initial exchangeable fraction becomes a target compartment when crops are either isolated from its Mg source by harvest, or, when Mg uptake comes to an end, for example during ripening of cereal crops. The 'apparent' difference in the Mg isotope composition between the crop and the remaining exchangeable fraction ( $\Delta^{26}$ Mg<sub>crop-rem. exch.</sub>, equation 3) represents an approximation of the crop uptake-related Mg isotope fractionation factor ( $\alpha^{26}$ Mg<sub>crop</sub>-<sub>rem. exch.</sub>), where the per mil expression of  $\alpha^{26} Mg_{crop-rem. exch.}$  is represented by  $\Delta^{26} Mg_{crop-}$  $_{\text{rem. exch.}} \sim 10^3 \cdot (\alpha^{26} \text{Mg}_{\text{crop-rem. exch.}} - 1)$ .  $\Delta^{26} \text{Mg}_{\text{crop-rem. exch.}}$  is assumed to remain constant throughout the crop's life cycle (Figure 2a,d) as indicated for Mg in a closed-system batch experiment by Black et al., (2008).

$$10^{3} \cdot \ln(\alpha^{26} \text{Mg}_{\text{crop-rem. exch.}}) \approx \Delta^{26} \text{Mg}_{\text{crop-rem. exch.}} \equiv \delta^{26} \text{Mg}_{\text{crop}} - \delta^{26} \text{Mg}_{\text{rem. exch.}}$$
 equation 3

The Mg isotope compositions of the target compartments also depend on the relative proportion of Mg taken up by crops to the Mg supplied to crops ( $f_{uptake}$ , equation 4), parametrized here by the Mg inventories in crops ( $I_{crop,t}^{Mg}$ ) and the initial exchangeable fraction of Mg in soil ( $I_{initial\ exch.}^{Mg}$ ). Thus,  $f_{uptake}$  can be understood as a measure of the Mg use efficiency of crops.

$$f_{uptake} = \frac{I_{crop,t}^{Mg}}{I_{initial \ exch.}^{Mg}} \label{eq:fuptake}$$
 equation 4

Importantly, to allow a quantitative representation of the partitioning of Mg isotopes among crop plants and the exchangeable fraction in soil, any Mg flux and soil-plant process beyond Mg uptake by crops and adsorption-desorption from the soil exchange complex is neglected for the time being (see section 3.3.2 for the consideration of further fluxes and processes). Also, sorption processes are assumed not to be subject to isotope fractionation as evidenced by previous isotope geochemical studies, in which the isotope composition of soil solution resembles the isotope composition of the exchangeable fraction (e.g., Wiegand et al., 2005; White et al., 2009; Bullen and Chadwick, 2016; Cai et al., 2022). In consideration of this simplification, a simple isotope mass balance equation can be established for this conceptual soil-plant system (equation 5).

$$\delta^{26} Mg_{initial\ exch.} = \delta^{26} Mg_{crop} \cdot f_{uptake} + \delta^{26} Mg_{rem.\ exch.} \cdot \left(1 - f_{uptake}\right) \hspace{1cm} \text{equation 5}$$

If the  $\delta^{26}$ Mg<sub>initial exch.</sub> value, f<sub>uptake</sub> and  $\Delta^{26}$ Mg<sub>crop-rem. exch.</sub> can be reasonably assumed, estimated or taken from literature, equation 3 to equation 5 enable the prediction of the Mg isotope compositions of crops ( $\delta^{26}$ Mg<sub>crop</sub> value, equation 6) and the exchangeable fraction ( $\delta^{26}$ Mg<sub>rem. exch.</sub> value, equation 7). This prediction allows a conceptual graphical representation of changes in the Mg isotope composition of crops and the exchangeable fraction of Mg in soils of various Mg inventories when simulating subsoil management (section 3.3.4, Figure 2).

$$\delta^{26} Mg_{crop} = \delta^{26} Mg_{initial \ exch.} + \Delta^{26} Mg_{crop-rem. \ exch.} \cdot \left(1 - f_{uptake}\right) \hspace{1cm} equation \ 6$$

$$\delta^{26} \text{Mg}_{\text{rem. exch.}} = \delta^{26} \text{Mg}_{\text{initial exch.}} - \Delta^{26} \text{Mg}_{\text{crop-rem. exch.}} \cdot f_{\text{uptake}}$$
 equation 7

#### 2.3.1. Implementation of a depth dependency to the exchangeable fraction

The aforementioned equations apply to the Mg isotope composition of bulk crop and the depth integral of the remaining exchangeable fraction of all soil horizons that contribute to crop nutrition. To predict the Mg isotope composition of the exchangeable fraction in soil of an individual soil horizon i that contributes to crop nutrition ( $\delta^{26}$ Mg<sub>rem. exch.,i</sub> value) and the Mg isotope composition of bulk crop that integrates Mg uptake across all these soil horizons ( $\delta^{26}$ Mg<sub>crop</sub> value) requires the introduction of a depth dependency in the aforementioned parameter  $f_{uptake}$ , and the  $\delta^{26}$ Mg values of the remaining exchangeable fraction in soil and bulk crop. As root density varies with soil depth, it can be assumed that Mg uptake from soil horizon i is proportional to the root density of this soil horizon. Consequently, the relative proportion of the root biomass in soil horizon i to that of the whole root ( $f_{root,i}$ ) can be used as a rough estimate for the contribution of soil horizon i to crop nutrition ( $f_{uptake,i}$ , equation 8).

$$f_{uptake,i} = \frac{I_{crop,t}^{Mg} \cdot f_{root,i}}{I_{constrain}^{Mg}}$$
 equation 8

Substituting  $f_{uptake}$  with  $f_{uptake,i}$  in equation 6 and equation 7 allows the calculation of the  $\delta^{26}Mg_{crop,i}$  value and the  $\delta^{26}Mg_{rem.\ exch.,i}$  value, respectively. Finally, the Mg isotope composition of bulk crop integrating Mg uptake from all soil horizons contributing to crop nutrition can be computed using equation 9.

$$\delta^{26} \text{Mg}_{\text{crop}} = \sum_{i=0}^{i} \delta^{26} \text{Mg}_{\text{crop},i} \cdot f_{\text{root},i}$$
 equation 9

#### 2.3.2. Consideration of further soil-plant processes affecting the $\delta^{26}$ Mg<sub>initial exch.</sub> value

The conceptual framework introduced above is valid in quantitative terms only, if i) the crop's Mg source is not replenished during crop growth, ii) Mg uptake by crops represents the only Mg isotope fractionating process, and iii) the  $\delta^{26} Mg_{\text{rem. exch.,i}}$  value set by Mg uptake from pre-crops (e.g., catch crops) is reset to the initial  $\delta^{26}$ Mg<sub>exch.,i</sub> value through Mg replenishment after pre-crop harvest. Obviously, all prerequisites are unlikely in a natural agricultural system that is much more complex than the conceptual isotope system introduced here as illustrated in Figure 1. Prerequisite i) is violated as the deposition of precipitation, and the solubilisation of soil constituents (e.g., SOM, soil minerals, organic and inorganic fertilizer, agricultural lime) and atmospheric dry deposition continues during crop growth. Even though mineral dissolution takes place without isotope fractionation beyond the stages of incipient weathering (Maher et al., 2016; Pokharel et al., 2019; Ryu et al., 2016, 2011; Wimpenny et al., 2010), which is also assumed for other soil constituents, the additional Mg would bias  $f_{uptake,i}$  and the  $\delta^{26}Mg_{initial\,exch.,i}$  value. Prerequisite ii) is violated too, if net neoformation of Mg-bearing secondary solids (Mg-clays, pedogenic Mg-carbonates) takes places. Prerequisite iii) depends on the turnover time of the exchangeable fraction with respect to replenishment. Fortunately, applying this concept to two adjacent plots of similar environmental and soil conditions with two soil management practices cancels out all confounding factors if consisting of: 1.) conventional soil management (control) causing shallow Mg uptake, 2.) subsoil management by physical melioration (e.g., deep loosening) (management) causing deeper Mg uptake than in the control. The magnitude of shifts in the  $\delta^{26} Mg_{crop}$  value and the  $\delta^{26} Mg_{rem. exch.,i}$  value among the control and management can then be expressed as  $\Delta_{crop}^{control-management}$  (equation 10) and  $\Delta_{\mathrm{exch,i}}^{\mathrm{control-management}}$  (equation 11), respectively.

$$\Delta_{crop}^{control-management} = \delta^{26} Mg_{crop}^{control} - \delta^{26} Mg_{crop}^{management} \qquad \qquad \text{equation 10}$$

$$\Delta_{\mathrm{exch,i}}^{\mathrm{control-management}} \!\! = \!\! \delta^{26} Mg_{\mathrm{exch,i}}^{\mathrm{control}} - \delta^{26} Mg_{\mathrm{exch,i}}^{\mathrm{management}}$$

equation 11

Finally, differences in the crop's Mg use efficiency among the management and the control can be obtained solely from the Mg isotope composition of the exchangeable fraction of a given soil horizon i by replacing the left-hand term of equation 11 with the respective right-hand terms of equation 7 and rearranging to  $f_{uptake,i}^{management} - f_{uptake,i}^{control}$  (equation 12). Negative values of  $f_{uptake,i}^{management} - f_{uptake,i}^{control}$  indicate an improvement in the Mg use efficiency as less Mg is required to obtain the same or higher grain yield, and *vice versa*.

$$f_{uptake,i}^{management} - f_{uptake,i}^{control} = \frac{\delta^{26} Mg_{exch,,i}^{control} - \delta^{26} Mg_{exch,,i}^{management}}{\Delta^{26} Mg_{crop-rem.\,exch.}}$$
 equation 12

#### 2.3.3. Input data for the graphical representation of the Mg isotope concept

Input data are required to graphically represent changes in the Mg isotope composition of crops and the exchangeable fraction of Mg in soil when simulating subsoil management. The selection of input data is presented next. In brief, input data include i) Mg inventories in crops at maturity stage ( $I_{crop,t_m}^{Mg}$ ) and the exchangeable fraction of Mg in soil ( $I_{initial\; exch.,i}^{Mg}$ ), ii) the soil horizon-specific proportions of Mg uptake ( $f_{root,i}$ ), and iii) the plant uptake-related 'apparent' Mg isotope fractionation factors ( $\Delta^{26}$ Mg<sub>crop-rem.exch.</sub>).

Inventory of Mg in crops ( $I_{crop,t_m}^{Mg}$ ) As agricultural studies are focused on grain and straw yield,  $I_{crop,t_m}^{Mg}$  is estimated from annual Mg offtakes (harvest yield + harvest residues) and the Mg inventory of crop residues remaining in soil after harvest. Thus,  $I_{crop,t_m}^{Mg}$  is obtained from equation 13, where  $I_{harvest\,yield}^{Mg}$  includes harvest yield such as grain, tuber, beet;  $I_{harvest\,residue}^{Mg}$  includes harvest residues such as straw, herb, leaf; and the correction factor 1.13 adds the Mg content of roots to the sum of harvest yield and harvest residues for non-beet crops. For the correction factor it is assumed that a relative proportion of root biomass to whole crop biomass, amounting globally to 13% (Chapin et al., 2012), represents the relative Mg content of roots to the whole crop. Certainly, this approach still over-simplifies ecological complexity as i) Mg is not uniformly proportioned among the crop organs, and ii) the Mg content in roots depends on the climatic regime, crop species, and the Mg availability in soil that can be enhanced if roots form symbiotic relationships with mycorrhizae. Aiming at accounting for these complicating factors, a minimum and maximum approach on  $I_{crop,t_m}^{Mg}$  is used in this study that is complemented by a sensitivity analysis (Supplementary Information 1) and assumed to suffice as a way

of conveying the concept. Minima and maxima of  $I_{harvest\,yield}^{Mg}$  and  $I_{harvest\,residue}^{Mg}$  were taken from Benker et al., (2016) for typical crops cultivated in Germany (e.g., cereal crops, legumes, beets, potatoes) and reported in Supplementary Information 2. Minima and maxima of  $I_{crop,t_m}^{Mg}$  used as input data for the isotope concept are 1.5 g m<sup>-2</sup>, representing the lower end for legumes, and 4.6 g m<sup>-2</sup>, representing the upper end for beets, respectively. For Oxisols the maximum of  $I_{crop,t_m}^{Mg}$  was set to 3.03 g m<sup>-2</sup> to avoid  $I_{initial\,exch.}^{Mg}$  running out of stock.

$$I_{crop,t_m}^{Mg} = 1.13 \cdot \left(I_{harvest \, yield}^{Mg} + I_{harvest \, residue}^{Mg}\right)$$
 equation 13

Inventory of Mg in the exchangeable fraction of soil horizon i ( $I_{initial\ exch,i}^{Mg}$ ). For  $I_{initial\ exch,i}^{Mg}$  Concentrations of the exchangeable fraction in soil (1M NH<sub>4</sub>OAc extraction) and soil density data was used from Alfisols, Andisols, Gelisols, Mollisols, Oxisols, Ultisols, and Vertisols according to the USDA Soil Taxonomy (Soil Survey Staff, 1999) for which these data were available. These soils represent soils with low, medium, and high inventories of exchangeable Mg. Input data are reported in Supplementary Information 3.

Soil horizon specific proportions of Mg uptake ( $f_{root,i}$ ). To simulate a change in the main Mg uptake depth caused by subsoil management, two scenarios of  $f_{root,i}$  were chosen. In the first scenario, which simulates the control,  $f_{root,i}$  of 70% was assigned to the topmost soil horizon (for thickness see Supplementary Information 3), which is consistent with the global compilation on crop rooting depth (Jackson et al., 1996). For simplicity, the remaining 30% were attributed to the subsequent soil horizon. In the second scenario, which simulates subsoil management in the soil horizon subsequent to the topmost soil horizon,  $f_{root,i}$  was doubled at the depth of subsoil management. Thus,  $f_{root,i}$  amounts to 40% at the topmost soil horizon and to 60% in the subsequent, managed soil horizon.

'Apparent' Mg isotope fractionation factor ( $\Delta^{26}Mg_{crop-rem.\,exch.}$ ) and the Mg isotope composition of the initial Mg source ( $\partial^{26}Mg_{initial\,\,exch.}$  value). Field-based plant uptake-related Mg isotope fractionation factors were not considered in this study as input parameters, as they require a detailed knowledge of all soil horizons contributing to plant nutrition, which is barely constraint in former Mg isotope studies. Of the few studies on the experimental determination of plant uptake-related Mg isotope fractionation factors, there are only two studies on crop plants. Whereas Black et al., (2008) determined a Mg isotope fractionation factor on wheat ( $\alpha^{26}Mg_{wheat-nutrient}$  = 1.00068), Wrobel et al., (2020) determined an 'apparent' Mg isotope fractionation factor on maize ( $\Delta^{26}Mg_{maize-nutrient}$  = 0.74‰). Consequently,  $\Delta^{26}Mg_{crop-rem.exch.} \sim 0.70\%$  was selected in this study. Compared with experimentally determined

 $\Delta^{26}$ Mg<sub>plant-source</sub> values of non-crop plants this value represents an upper limit of  $\Delta^{26}$ Mg<sub>plant-source</sub> and was thus used as maximum estimate of  $\Delta^{26}$ Mg<sub>crop-rem. exch.</sub> The minimum estimate of  $\Delta^{26}$ Mg<sub>crop-rem. exch.</sub> was set as half of the maximum estimate. A sensitivity analysis provided in Supplementary Information 1 illustrates how Mg isotope shifts vary with variations in  $\Delta^{26}$ Mg<sub>crop-rem.exch.</sub> beyond the range of minima and maxima values of  $\Delta^{26}$ Mg<sub>crop-rem. exch.</sub> For simplicity, the Mg isotope composition of the initial Mg source ( $\delta^{26}$ Mg<sub>initial exch.</sub> value) was set here to a value of 0.00‰.

#### 2.3.4. Magnesium isotope shifts for simulated subsoil management

The central question is whether a deepening of the crop's main Mg uptake depth caused by subsoil management (e.g., deep loosening) has the potential to shift Mg isotope ratios in crops and the exchangeable fraction of Mg in soil to a magnitude that can be resolved from the uncertainty of Mg isotope analyses (error propagated long-term external precision amounting to  $\sim$ 0.11‰ per amu at the two-fold standard deviation level, Supplementary Information 4). By applying minima and maxima input parameters ( $I_{crop,t_m}^{Mg}$ ,  $\Delta^{26}Mg_{crop-rem.\,exch.}$ ) along with the set of equations provided above enables now a conceptual graphical representation of changes in the Mg isotope composition of crop plants, and the exchangeable fraction of Mg in soil horizon i when simulating subsoil management for soils with low, medium and high inventories of exchangeable Mg in Figure 2 (output data summarized in Supplementary Information 3).

Conceptual Figure 2b-c,e-f demonstrates that  $\Delta_{\text{exch.,i}}^{\text{control-management}}$ , ranging from -0.09% to 0.35%, is larger than  $\Delta_{\text{crop}}^{\text{control-management}}$ , ranging from -0.02% to 0.25%, and deepening the main Mg uptake depth results in more negative  $\delta^{26}$ Mg<sub>exch.i</sub> values. Considering minimum estimates of  $I_{\text{crop,t_m}}^{\text{Mg}}$  and  $\Delta^{26}$ Mg<sub>crop-rem.exch</sub>. Mg isotope shifts beyond the uncertainty of Mg isotope analyses were only found for Oxisols ( $\Delta_{\text{exch.,i}}^{\text{control-management}}$ : 0.09%) (Figure 2b-c). When considering maximum estimates of  $I_{\text{crop,t_m}}^{\text{Mg}}$  and  $\Delta^{26}$ Mg<sub>crop-rem.exch</sub>, these shifts become more pronounced and occur in different soils (Figure 2e-f). For example, Mg isotope shifts beyond the uncertainty of Mg isotope analyses are lowest for Andisols ( $\Delta_{\text{exch.,i}}^{\text{control-management}}$ : 0.25%,  $\Delta_{\text{crop}}^{\text{control-management}}$ : 0.12%) and highest for Oxisols ( $\Delta_{\text{exch.,i}}^{\text{control-management}}$ : 0.35%,  $\Delta_{\text{crop}}^{\text{control-management}}$ : 0.25%). The reason why the exchangeable fraction is more sensitive to Mg isotope shifts induced by subsoil management than crops is because crops integrate Mg uptake over two or more soil horizon whereas the exchangeable fraction keeps its *in situ*  $\delta^{26}$ Mg value. As a rule of thumb, the more soil horizon involved in crop nutrition, the less pronounced potential Mg isotope shifts will be. This concept will next be tested in field trials for Alfisols, which correspond to Luvisols (IUSS Working Group WRB 2015) in the field trials of this study.

#### 3. Materials and methods

#### 3.1. Field site

The field study was conducted at the Experimental Station of the University of Bonn "Campus Klein-Altendorf" located in Rheinbach (6° 59' 29" E, 50° 37' 21" N). The climate is temperate and humid with a long-term (1956 to 2014) mean annual temperature (MAT) of 9.4°C and mean annual precipitation (MAP) of 603 mm. The soil is classified as Haplic Luvisol (hypereutric, siltic) developed from loess (IUSS Working Group WRB 2015), and is characterized by a silty clay loam texture with clay accumulation in the subsoil between 45 and 95 cm soil depth. The CaCO<sub>3</sub> content is <1 g kg<sup>-1</sup> from 0 – 1.27 m soil depth and rises to 1.27 g kg<sup>-1</sup> below 1.27 m depth (Barej et al., 2014). The bulk soil density increases from 1.29 g cm<sup>-3</sup> to 1.52 g cm<sup>-3</sup> from topsoil to 1 m soil depth (Barej et al., 2014). For a more detailed description of the soil the reader is referred to Barej et al., (2014).

#### 3.2. Experimental field trial and subsoil management

Field experiments were conducted at three central field trials (CF), namely CF 1-1, CF 1-2, and CF 2. Each central field trial was subdivided into single plots allowing various subsoil management methods complemented by a control with three field replicates at CF 1-1 and CF 1-2, and four field replicates at CF 2. A detailed description on the technical realization of subsoil management is given in Jakobs et al., (2019), Hinzmann et al., (2021), and Schmittmann et al., (2021). In brief, subsoil management was carried out by strip-wise melioration in September of the respective starting year (CF 1-1: 2016, CF 1-2: 2017, CF 2: 2019) and included i) deep loosening (DL); ii) deep loosening with the incorporation of biowaste compost (DLB) from kitchen waste of private households, or green waste compost (DLG) from trees, bushes and shrubs of public green spaces and parks; iii) deep loosening with biowaste compost in combination with the deep rooting pre-crop lucerne (DLB luc.). Quantities of incorporated organic material amount to 5 kg m<sup>-2</sup> (DLB) at CF 1-1; 3 kg m<sup>-2</sup> (DLB min.), 5 kg m<sup>-2</sup> (DLB mid.), 7 kg m<sup>-2</sup> (DLB max.), and 5 kg m<sup>-2</sup> (DLG) at CF 1-2; and 3 kg m<sup>-2</sup> (DLB) at CF 2. Lucerne was regularly harvested and mulched in 2018. Deep loosening was applied to a depth of 60 cm, and organic material was incorporated at a depth of 30-60 cm at CF 1-1 and CF 1-2, and at 30-45 cm at CF 2. Prior to the subsoil management all central field trials were limed with converter lime (Lhoist Germany, Rheinkalk GmbH) in 2015 (0.3 kg m<sup>-2</sup>) and 2016 (0.4 kg m<sup>-2</sup>) and annually fertilized with ~30 g m<sup>-2</sup> calcium ammonia nitrate (CAN). After subsoil management mustard was sown at both field trials as catch crop and mulched prior to performing a crop rotation in the order of spring barley (CF 1-2: 2018, CF 2: 2020) followed by winter wheat (CF 1-1: 2018, CF 1-2: 2019).

#### 3.3. Sampling and sample preparation

Winter wheat (*Triticum aestivum L.*) was sampled at flowering stage in 2018 (CF 1-1) and maturity stage in 2019 (CF 1-2). Spring barley (*Hordeum vulgare L.*) was sampled at flowering stage in 2018 (CF 1-2), in 2020 (CF 2), and at maturity stage in 2018 (CF 1-2). Only aboveground shoots of winter wheat and spring barley were collected. The reason for omitting roots from sampling is that only the topmost part of the roots was removable from the hardened topsoil. Thus, root biomass would have been sampled incompletely. Representative aliquots of biowaste and green waste compost were taken in 2016 at CF 1-1 only.

Soil sampling was performed on the same day of crop sampling beneath the sampled shoot. At CF 1-1 and CF 1-2 soil samples were collected from soil cores taken with a soil auger of 6 cm inner diameter lined with an inner plastic sleeve for sample recovery. At CF 2 soil samples were taken from freshly excavated soil pits. Composite soil samples of the respective soil horizon were taken to 1 m depth. Specifically, the depth intervals of 0-30 cm (Ap horizon), 30-50 cm (E/B horizon), 50-60 cm (Bt1 horizon), 60-70 cm (Bt2 horizon), 70-100 cm (Bt3 horizon) were sampled at CF 1-1 and CF 1-2. At CF 2 the open soil pit allowed for a higher sampling resolution from 0-10 cm (Ap horizon), 10-20 cm (Ap horizon), 20-30 cm (Ap horizon), 30-45 cm (E/B horizon), 45-60 cm (Bt1 horizon), 60-80 cm (Bt2 horizon), 80-100 cm (Bt3 horizon). An aliquot of converter lime of a batch from 2021 (Lhoist Germany, Rheinkalk GmbH) was collected because reference samples from 2015–2016 were consumed for previous analyses.

Both plant and soil samples were transferred from field to laboratory on the day of sampling and frozen at -20°C. Prior to soil sieving (<2 mm fraction), or dissection of plant samples into whole ear, stem and leaves, samples were dried by lyophilization for a minimum of 24 hr at -55°C using a Christ Beta 1-8LD plus freeze drier (Martin Christ Gefriertrocknungsanlagen GmbH, Germany). Aliquots of compost and converter lime were dried in an oven for 24 hr at 60°C. Plant organs were milled in 100 ml sealable HDPE bottles equipped with tungsten carbide milling balls using a shaker (Collomix Agia 330, Collomix GmbH, Germany). To minimize analytical effort and costs, particularly on the analyses of Mg stable isotopes, the field replicates of soil samples were pooled and homogenized using a rotator overhead shaker (BioSan Multi Bio RS-24, Germany). Any potential form of natural heterogeneity is accounted for by field replicates of plant samples.

#### 3.4. Analytical methods

Soil digestion using Li<sub>2</sub>B<sub>4</sub>O<sub>7</sub> fusion and the analyses of element concentrations using inductively coupled plasma optical emission spectroscopy (ICP-OES, iCAP 6500, Thermo Scientific, Germany) was performed at the Central Institute of Engineering, Electronics and Analytics (ZEA-3) of Forschungszentrum Jülich GmbH. The remaining analytics comprising microwave assisted sample

digestion, element concentration analyses by quadrupole inductively coupled plasma mass spectrometry (ICP-MS, Agilent 7900, Agilent Technology Inc., United States), analyses of soil pH, loss on ignition, and Mg isotope ratios were performed at the Institute of Bio- and Geosciences (IBG-3) at Forschungszentrum Jülich GmbH that is equipped with a self-made, low particulate clean laboratory.

#### 3.4.1. Sample digestion and concentration analyses

*Plant and compost samples.* A maximum of 400 mg of powdered and homogenized whole ears, stems, leaves, or compost were digested using a pressurized microwave digestion system (turboWAVE, Milestone Srl, Italy) and a mixture comprising 3.5 ml 15M HNO<sub>3</sub>, 2 ml 30%  $H_2O_2$  and 2.5 ml deionized water (18.2 MΩ cm, TOC < 3 ng g<sup>-1</sup>, Merck Millipore, Germany). Plant digests were centrifuged at 8000 rpm for 5 min (Beckman-Coulter Allegra X30R, USA, equipped with a fixed-angle rotor (F0685), 25°,  $r_{max}$  = 97 mm) to separate the dissolved sample from silicate residues and the supernatant was pipetted off. The residuum was rinsed three times each with 1 ml deionized water, centrifuged and the supernatants were combined to ensure the complete transfer of the dissolved sample. Magnesium concentrations were analysed by ICP-OES following the Cs-HNO<sub>3</sub> method described in Schuessler et al., (2016). Procedural blanks were processed with each sample batch and results were below the limit of quantification (LOQ). Relative uncertainties, given as the relative deviation of the measured element concentration of a standard reference material (SRM) to its certified value, were assessed by processing NIST SRM 1515 apple leaves with each sample digestion batch and by processing NIST SRM 1573a tomato leaves, NIST SRM 1575a pine needles and ERM-CD281 rye grass occasionally. Relative uncertainties are reported in Table S5 and amount to better than ±10%.

Bulk soil and converter lime samples. Prior to digestion a representative aliquot of 1 g of pooled and homogenized soil was milled using an agate mortar and pestle. Then, fusion digestion was performed by mixing 50 mg of soil with 250 mg of Li<sub>2</sub>B<sub>4</sub>O<sub>7</sub> followed by heating at 1050°C for 30 min in a muffle furnace. Magnesium concentrations, expressed as oxide concentrations, were analysed by ICP-OES. Loss on ignition (LOI) was determined by heating 0.5 g of soil at 550°C for 2h in a muffle furnace to rescale element concentrations to 100%. The complete digestion of soil does not represent natural mineral dissolution processes as quartz, for example, is resistant to chemical weathering. Hence, to better represent chemical weathering another soil aliquot was exposed to a strong acid extraction using the same microwave assisted digestion method as for plant samples and a maximum of 50 mg soil. An aliquot of 50 mg of converter lime was dissolved in 6M HCl, evaporated to dryness and redissolved in 0.3M HNO<sub>3</sub>. Magnesium concentrations of microwave digests and converter lime were analysed by ICP-MS. Procedural blanks were processed with each sample batch and results were below the LOQ. Relative uncertainties of the fusion digestion were assessed by repeat digestion of NIST SRM

2709a San Joaquin soil and amount to better than ±5% as reported in Table S1b. The extraction recovery (calculated from the concentration ratio between microwave digests and fusion digests) is about 90% (Table S2b) and is comparable for soil samples of this study and SRM 2790a (not shown).

#### 3.4.2. Exchangeable fraction in soil

The exchangeable fraction of Mg in soil was extracted by adapting extraction methods from Arunachalam et al., (1996) and Bolou-Bi et al., (2012). Two grams of dried and sieved soil (<2 mm fraction) were suspended in 20 ml of 1M NH<sub>4</sub>OAc, and gently shaken for 2 hr using a rotator overhead shaker (BioSan Multi Bio RS-24, Germany). The suspension was centrifuged at 8000 rpm for 5 min, and the supernatant was passed through pre-rinsed 0.20  $\mu$ m acetate filter. Magnesium concentrations were measured by ICP-MS. Procedural blanks were processed with each sample batch and results were below the LOQ. Relative uncertainties were assessed by repeat analyses of NIST SRM 1640a natural water that is appropriate to resemble the sample matrix of the exchangeable fraction in soil and amounted to better than  $\pm 5\%$  (Table S4).

#### 3.4.3. Soil pH

An aliquot of 1 g dried and sieved soil (<2 mm fraction) was suspended in 5 ml 0.01M CaCl<sub>2</sub>, shaken for 20 min using a rotator overhead shaker (BioSan Multi Bio RS-24, Germany) and centrifuged at 8000 rpm for 5 min. The soil pH was measured in the supernatant using a Mettler Toledo pH Meter (MP 220). The reproducibility of soil pH measurements was estimated from repeat analyses of NIST SRM 2709a San Joaquin and amounted to 0.2 (2SE, N=9, Table S3).

#### 3.4.4. Cation-exchange chromatography and Mg isotope analysis

Purification of Mg from matrix elements was done using two cation-exchange chromatography methods. Both methods were adapted from published protocols to separate Mg from three different sample matrices, namely plant matrix (calibrated using NIST SRM 1515 apple leaves), soil matrix after microwave digestion (calibrated using NIST SRM 2709a San Joaquin soil), and soil solution matrix representing the 1M NH<sub>4</sub>OAc soil extraction (calibrated using NIST SRM 1640a natural water) with the same chromatography method. In the first method, adapted from Wombacher et al., (2009), a sample aliquot containing 20 μg Mg was loaded onto converted, disposable, 7.5 ml Pasteur pipettes fitted with a polypropylene frit and packed with 3.1 ml AG50W-X8 resin (200-400 mesh, Bio-Rad). Matrix elements (K, Na) were eluted with 90 ml 0.4M HCl and Mg was eluted with 22 ml 1.5M HCl, evaporated to dryness and redissolved in 0.2 ml 0.7M HCl. In the second method, adapted from Bohlin et al., (2018), the pre-purified Mg was loaded onto 15 ml Savillex © micro columns packed with 3.1 ml AG MP 50 resin (100-200 mesh, Bio-Rad). Matrix elements were eluted with 3 ml 0.5M HF, 41 ml 0.7M

HCl, 1 ml 1.5M HCl, and Mg was eluted with 10 ml 1.5M HCl. The remaining matrix was eluted with 60 ml 6M HCl. Each resin-packed column was re-used about twenty times. Pure Mg solutions were evaporated to dryness, redissolved in a 1:1 (v/v) mixture of 15M HNO<sub>3</sub> and 30%  $H_2O_2$  and heated at 150°C for 4h to oxidise organic compounds that would otherwise cause isobaric interferences during mass spectrometry. Aliquots were taken to check the Mg recovery, blank contribution, and purity. The Mg recovery was typically better than 99.7% and the blank contribution typically amounted to less than 1%. Impurities (given in % relative to Mg) were either caused by co-eluting transition metals such as Co (typically  $\leq$ 10%, but also up to 60%), Cu ( $\leq$ 10%), Zn ( $\leq$ 15%) in plant samples and elements tailing into the Mg peak like Fe ( $\leq$ 140%), Ni ( $\leq$ 1%), Mn ( $\leq$ 2%) in soil samples, or by blank contribution (Ca  $\leq$ 5%) during evaporation of the pure Mg solution. Matrix doping experiments (Appendix B) were performed to ensure that impurities above the commonly accepted  $\leq$ 5% impurity level (Tipper, 2022) do not bias accuracy and precision of Mg isotope analyses.

Magnesium isotopes were measured by multi-collector ICP-MS (Nu Plasma II, Nu Instruments Ltd, United Kingdom) in wet plasma mode at low mass resolution in 0.3M HNO<sub>3</sub> at a typical sensitivity of 17-20 V/ppm on mass 24. The standard-sample-standard bracketing method was applied by using the "new"  $\delta$ -zero bracketing standard ERM-AE143 (Vogl et al., 2020). Given that Fe impurities accounted for up to 140% in purified soil digests, ERM-AE143 was doped with Fe to match the Fe/Mg ratio of the respective sample. Results are expressed as the ‰ difference of the Mg isotope ratio of the sample relative to ERM-AE143 using the delta notation:  $\delta^{x}$ Mg=[( $^{x}$ Mg/ $^{24}$ Mg)<sub>sample</sub>/( $^{x}$ Mg/ $^{24}$ Mg)<sub>ERM-AE143</sub>-1]·1000, where x refers to either 26 or 25.  $\delta^{x}$ Mg<sub>ERM-AE143</sub> values were converted to the DSM-3 scale using the conversion factors -3.284‰  $\pm$  0.027‰ for  $\delta^{26}$ Mg values and -1.681‰  $\pm$  0.021‰ for  $\delta^{25}$ Mg values (Vogl et al., 2020) following equation 2 in Young and Galy (2004).

Accuracy and precision were assessed by processing ERM-AE143 ( $\delta^{26}$ Mg = -3.26%  $\pm$  0.07%, N=19) with each sample batch through the cation-exchange chromatography method and by analysing them in the same sequence as samples. To also account for sample matrix and sample digestion NIST SRM 1515 apple leaves ( $\delta^{26}$ Mg = -1.16%  $\pm$  0.05%, N=19), NIST SRM 2709a San Joaquin soil ( $\delta^{26}$ Mg = -0.11%  $\pm$  0.06%, N=7) and NIST SRM 1640a ( $\delta^{26}$ Mg = -0.64%  $\pm$  0.07%, N=5) were processed with each sample batch to assess the accuracy and precision of the full analytical procedure. The Mg isotope compositions of all reference materials agree with previously reported values (Figure 3) and are summarised together with those reference materials (NIST SRM 1573a tomato leaves, NIST SRM 1575a pine needles, ERM-CD281 rye grass, 1M NH<sub>4</sub>OAc soil extraction of NIST SRM 2709a San Joaquin soil), which were occasionally processed, in Tables S2b, S4 and S5. The long-term external precision over the course of 36 months was estimated to be  $\pm$ 0.07% (2SD) for  $\delta^{26}$ Mg being in line with the compiled value of 0.08% (Supplementary Information 4).

#### 3.5. Computational methods

#### 3.5.1. Magnesium concentrations of shoots and whole crop

The Mg concentration of bulk shoot ( $[Mg]_{shoot}$ ) or whole crop ( $[Mg]_{whole\,crop}$ ) was calculated from equation 14, where j refers to the crop organs ear, stem, leaf, or root and f denotes the relative proportion of the dry biomass of the respective crop organ j to the total dry biomass of the shoot or the whole crop.

$$[Mg]_{shoot \text{ or whole crop}} = \sum_{j=\text{organ}}^{j} [Mg]_{j} \cdot f_{j}$$
 equation 14

#### 3.5.2. Magnesium isotope composition of shoots and whole crop

The Mg isotope composition of shoots ( $\delta^{26}$ Mg<sub>shoot</sub> value) or whole crop ( $\delta^{26}$ Mg<sub>whole crop</sub> value) was calculated from equation 15, where  $\delta^{26}$ Mg refers to the Mg isotope composition of the crop organ j.

$$\delta^{26} \text{Mg}_{\text{shoot or whole crop}} = \sum_{j=\text{organ}}^{j} \delta^{26} \text{Mg}_j \cdot [\text{Mg}]_j \cdot f_j \bigg/ \sum_{j=\text{organ}}^{j} [\text{Mg}]_j \cdot f_j$$
 equation 15

Roots were not sampled in this study (section 4.3). Instead, f<sub>root</sub> and [Mg]<sub>root</sub> used in equation 14 and equation 15, and the difference in the Mg isotope composition between root ( $\delta^{26}$ Mg<sub>root</sub> value) and stem ( $\delta^{26}$ Mg<sub>stem</sub> value) expressed as  $\Delta^{26}$ Mg<sub>root-stem</sub> were compiled from the few Mg isotope studies on crops that include root analyses and reported in Supplementary Information 5. As the  $\delta^{26} Mg_{root}$  value depends on the  $\delta^{26}$ Mg value of the respective nutrient source,  $\Delta^{26}$ Mg<sub>root-stem</sub> was chosen to calculate the  $\delta^{26} Mg_{root}$  value of the crops of this study. Given the lack of Mg isotope studies on winter wheat and spring barley cultivated under similar environmental conditions to that in this study, the compiled data may not be fully representative for the crops collected in this study. However, within uncertainty (standard error (SE) of the mean value)  $\Delta^{26}$ Mg<sub>root-stem</sub>, [Mg]<sub>root</sub> and f<sub>root</sub> likely matched the unsampled roots of this study. Data were compiled from Bolou-Bi et al., (2010) for ryegrass and clover grown hydroponically and in a phlogopite mineral culture, Gao et al., (2018) for rice cultivated in the field, Wang et al., (2021) for rye cultivated in the field, and Wang et al., (2020) for winter wheat at flowering and maturity stage grown in a quartz mineral culture. The mean values and standard errors across these studies were:  $\Delta^{26}$ Mg<sub>root-stem</sub> = 0.27 ± 0.05%, [Mg]<sub>root</sub> = 734 ± 157 µg g<sup>-1</sup> and f<sub>root</sub> = 15 ± 3%. To account for differences in the relative proportion of root biomass and growing stage among crop species, two root scenarios were considered. In the first root scenario the average value of root biomass from the aforementioned compilation (15 ± 3%) was used and is considered as a minimum estimate at flowering stage (hereafter termed '15% root scenario'). In the second root scenario 40% root biomass was chosen and considered as a maximum estimate at flowering stage (hereafter termed '40% root scenario') (Beißmann, 2021). For samples collected at maturity stage, a root mortality of 50% occurring from flowering to maturity stage was assumed.

#### 4. Results

#### 4.1. Chemical composition of soil and shoots

The soil pH (0.01M CaCl<sub>2</sub>, Figure 4d, h, l, p, Table S3) ranged from 6.6 to 8.1, thus provided near optimum conditions for the bioavailability of Mg. In all control plots, the soil pH barely changed with soil depth. In contrast, the incorporation of biowaste compost increased the soil pH only at CF 2 (DLB) at the depth of compost incorporation and below (Figure 4p), which agrees with a previous study by Odlare et al., (2008).

Magnesium concentrations of bulk shoots (Figure 4a, e, i, m, Table 2) in all control and management plots were identical within uncertainty obtained from field replicates. Magnesium concentrations of bulk soil (Figure 4c, g, k, o, Table S1a, b Table S2a, b) increased with depth at all field trials. Management effects were not evident for bulk soil because differences beyond the analytical uncertainty were attributed to heterogeneity in the field as indicated by shoots. Magnesium concentrations of the exchangeable fraction (1M NH<sub>4</sub>OAc extraction, Figure 4b, f, j, n, Table S4) in the soil of the control followed the trend of those in bulk soil. The relative proportion of Mg in the exchangeable fraction to bulk soil amounted on average to about 2.3%, suggesting that only a minor fraction of Mg in soil was bioavailable. However, management effects towards increased Mg concentrations were evident only at CF 1-1 at the depth of biowaste compost incorporation and above, and at CF 2 at the depth of biowaste compost incorporation.

#### 4.2. Magnesium isotope composition of soil-plant compartments

The most positive  $\delta^{26}$ Mg values in this study were found for microwave digested bulk soil ( $\delta^{26}$ Mg<sub>soil</sub> values, Figure 5, Table S2b, see Appendix C for the lack of isotope effects on incomplete sample digestion) with  $\delta^{26}$ Mg<sub>soil</sub> = 0.08 ± 0.10‰ (mean ± 2SD, N=83). This value was isotopically heavier than the bulk silicate Earth (-0.25 ± 0.07‰, Teng et al., (2010)) most likely due to differential weathering in the geologic past that was not recorded any longer in the exchangeable fraction in soil because its turnover time amounts typically to  $10^3$  - $10^5$  years. No systematic variation of  $\delta^{26}$ Mg<sub>soil</sub> values were found along the depth profile or among the field trials of the control and management.

The most negative  $\delta^{26} Mg$  values in this study were found for the exchangeable fraction of Mg in soil ( $\delta^{26} Mg_{exch.}$  values, Figure 5b-c, e-g, i-k, m-o, Table S4) and in converter lime ( $\delta^{26} Mg_{lime}$  value, Figure 5, Table S2b) with  $\delta^{26} Mg_{exch.} = -1.27 \pm 0.28\%$  (mean  $\pm$  2SD, N=83) and  $\delta^{26} Mg_{lime} = -1.38$ 

 $\pm$  0.07‰.  $\delta^{26}$ Mg<sub>exch.</sub> values followed a shallow bulge shape with soil depth. Specifically,  $\delta^{26}$ Mg<sub>exch.</sub> values shifted to more positive values from topsoil to 50 cm soil depth and then declined to more negative  $\delta^{26}$ Mg values at the bottom of the soil profile. Deep loosening (DL) or using lucerne as pre-crop (C luc.) had no effect on  $\delta^{26}$ Mg<sub>exch.</sub>values. However, the incorporation of biowaste compost (DLB) or green waste compost (DLG) resulted in shifts in  $\delta^{26}$ Mg<sub>exch.</sub> values towards more positive  $\delta^{26}$ Mg<sub>exch.</sub> values, which was most pronounced for DLB at the depth of compost incorporation (Figure 5c, n).

The Mg isotope compositions of shoots ( $\delta^{26}$ Mg<sub>shoot</sub> values, Figure 5 b-c, e-g, i-k, m-o, Figure 6af, Table 2), and biowaste and green waste compost ( $\delta^{26}$ Mg<sub>biowaste compost</sub> value,  $\delta^{26}$ Mg<sub>green waste compost</sub> value, Figure 5, Table S5) lay between  $\delta^{26} Mg_{soil}$  and  $\delta^{26} Mg_{exch.}$  values with  $\delta^{26} Mg_{shoot} = -0.83 \pm 0.21\%$ (mean  $\pm$  2SD, N=25),  $\delta^{26}$ Mg<sub>biowaste compost</sub> = -0.47  $\pm$  0.02‰, and  $\delta^{26}$ Mg<sub>green waste compost</sub> = -0.51  $\pm$  0.04‰. The mean  $\delta^{26} Mg_{shoot}$  values of winter wheat ( $\delta^{26} Mg_{wheat shoot} = -0.73 \pm 0.12\%$ , N=8) and spring barley  $(\delta^{26}Mg_{barley shoot} = -0.88 \pm 0.18\%, N=17)$  were identical within uncertainty. It is worth noting that even at a maximum content of Mg in roots (40% root scenario, section 4.5.2)  $\delta^{26}$ Mg<sub>whole crop</sub> values would shift from the  $\delta^{26}$ Mg<sub>shoot</sub> values only either by 0.10% towards more positive or by 0.06% towards more negative  $\delta^{26}$ Mg values (Figure 5a, d, h, l), which is within the error propagated uncertainty (Table 2). Among the individual crop organs (Figure 6a-e, Table S5)  $\delta^{26}$ Mg values of leaves and stems were isotopically the lightest shoot organs and comparable one another, while ears, dominating the  $\delta^{26} Mg_{shoot}$  value by means of Mg content, were isotopically the heaviest shoot organ. The intra-crop differences were consistent with previous isotope studies on crops (e.g. Gao et al., (2018) on rice, Wang et al., (2021) on winter rye, Black et al., (2008) and Wang et al., (2020) on winter wheat) and will not be discussed in this article. However, effects of subsoil management on  $\delta^{26} Mg$  values of bulk shoots were unresolvable from uncertainties except for DLB mid. (Figure 6e), where the  $\delta^{26}$ Mg value of bulk shoot next to the melioration strip (side) was isotopically lighter than the  $\delta^{26}$ Mg value of the shoot on the melioration strip (strip). Disregarding uncertainties this systematic was also found for DLB min. and DLB max. (Figure 6e).

#### 5. Discussion

The Mg isotope compositions of bulk crop ( $\delta^{26}$ Mg<sub>crop</sub> value) and the exchangeable fraction of Mg in soil ( $\delta^{26}$ Mg<sub>exch.</sub> value) from the field trials suggest weak but systematic differences among the control and the subsoil managed plots. Whether these differences can solely be attributed to a change in the Mg use efficiency at depth caused by subsoil management will be evaluated next.

#### 5.1. Evaluation of Mg isotope shifts among the control and subsoil managed plots

Luvisols (IUSS Working Group WRB 2015) correspond to Alfisols in the USDA Soil Taxonomy (Soil Survey Staff, 1999). Thus, the results found at the DL managed plots of this study can now be compared with the outcome of the conceptual framework on the magnitude of Mg isotope shifts in crops and the exchangeable fraction of Mg in soil among a control and a subsoil managed soil ( $\Delta_{\rm crop}^{\rm control-management}$ ,  $\Delta_{\rm exch.,i}^{\rm control-management}$ ) simulated for DL without compost incorporation. At the field trials of this study  $\Delta_{\rm crop}^{\rm control-management}$  and  $\Delta_{\rm exch.,i}^{\rm control-management}$  cannot be resolved from the uncertainty of Mg isotope analyses of about 0.11% (Supplementary Information 4). This finding agrees with the predictions made for Alfisols and can be attributed to a reservoir effect (e.g., Tipper et al., 2012), namely to the large inventory of Mg stored in the exchangeable fraction of the soil (e.g., Spohn et al., 2021; Cai et al., 2022).

In contrast, DL combined with compost incorporation resulted in  $\Delta^{control-management}_{exch.,i}$  of up to -0.19‰ at the depth of compost incorporation and to about -0.12‰ in the topsoil (e.g., Figure 5c). Even though these Mg isotope shifts were resolvable from the uncertainty of Mg isotope analyses they exceeded by far the predicted  $\Delta_{\mathrm{exch},i}^{control-management}$  value of about -0.01‰ to 0.02‰ for Alfisols (Supplementary Information 3). Thus,  $\Delta_{\mathrm{exch,i}}^{\mathrm{control-management}}$  cannot be solely attributed to plant uptake-related isotope fractionation. Instead, a modification of the exchangeable fraction by isotopically distinct, compost-derived Mg (Figure 5c) is likely; for example, due to compost decomposition followed by the entry of compost-derived Mg in the exchangeable fraction. This effect was also found in the topsoil horizon, albeit less pronounced, possibly due to a carryover effect from depth to the surface during compost incorporation, or nutrient uplift (Jobbágy and Jackson, 2004) within only two few years from compost incorporation in 2016 to sampling in 2018. An indication for nutrient uplift was indeed found in spring barley cultivated on the DLB mid. meliorated strip (strip) and next to it (side) (Figure 6e) because  $\Delta_{crop}^{control-management}$  amounting to -0.21% (Table 2) also exceeded the predicted maximum  $\Delta_{crop}^{control-management}~$  value of 0.01% (Supplementary Information 3). As deep loosening generally reduces root penetration resistance and thus results in increases in root length density (Jakobs et al., 2019; Schneider et al., 2021), the isotopically heavier shoots of spring barley on the strip confirm, despite the lack of soil samples at these plots, the uplift of isotopically distinct compost-derived Mg from greater depth than on the non-managed site.

#### 5.2. Crop uptake-related 'apparent' Mg isotope fractionation factor

Isotope fractionation factors are key to quantify the partitioning of Mg stable isotopes among soilplant compartments. Isotope fractionation factors can be determined theoretically from vibrational frequencies using *ab initio* calculations as done, for example, for Fe and Ca isotopes for plant uptake (Moynier et al., 2013; Moynier and Fujii, 2017b) and for Mg isotopes between chlorophylls (Moynier and Fujii, 2017a). However, plant uptake-related Mg isotope fractionation factors are typically empirically determined by experiments (e.g., Black et al., 2008; Bolou-Bi et al., 2010) or from field samples (e.g., Bolou-Bi et al., 2012, Opfergelt et al., 2014, Kimmig et al., 2018). A prerequisite of the latter is that plant uptake represents the only process that fractionates Mg isotopes, which is argued to be the case in this study by three lines of evidence. First, neoformation of Mg-bearing secondary minerals can be excluded for the soils of this study based on X-ray diffraction analyses that revealed vermiculite as the only Mg containing clay mineral (Vetterlein et al., 2013) – a mineral that is formed by mineral transformation processes rather than from precipitation from an oversaturated solute. Second, the net formation of Mg-carbonates can be ruled out, as in this case the Mg isotope composition of the exchangeable fraction in soil would be isotopically heavy but not lighter as in this study. Third, given the advanced degree of chemical depletion in Luvisols, incipient weathering and differential weathering of highly soluble and isotopically light minerals (e.g., primary chlorite that can be about 1‰ isotopically lighter than its host bulk rock (Ryu et al., 2011)) can also be excluded.

Field-based plant uptake-related isotope fractionation factors require the knowledge on the soil horizons contributing to crop nutrition, if the  $\delta^{26}Mg_{rem. exch.}$  value strongly varies with depth. The latter is not the case in this study (Figure 5b-c, e-g, i-k, m-o). Thus, an 'apparent' fractionation factor  $(\Delta^{26} Mg_{crop-rem. exch.})$  was calculated using equation 3 from the Mg isotope composition of bulk crops (15% root scenario) and the depth integral of the Mg isotope composition of the remaining exchangeable fraction in soil that was weighted by its Mg inventories using samples from the control and the DL plots without compost incorporation. The resulting averaged (mean ± 2SD, N=4) plant uptake-related apparent Mg isotope fractionation factors amount to  $\Delta^{26}$ Mg<sub>wheat-rem.exch.</sub> = 0.63 ± 0.05% and  $\Delta^{26}$ Mg<sub>barley-</sub> <sub>rem. exch.</sub> = 0.37  $\pm$  0.12%. Assuming that the estimation of the  $\delta^{26}$ Mg<sub>root</sub> value of unsampled roots correctly converts the  $\delta^{26}$ Mg<sub>shoot</sub> value of sampled shoots to its  $\delta^{26}$ Mg<sub>whole crop</sub> value, the plant uptakerelated apparent Mg isotope fractionation factors are seemingly species-dependent. These fractionation factors agree well with the lower and upper limit of  $\Delta^{26}$ Mg<sub>crop-rem. exch.</sub> (0.35% and 0.70%, section 3.3.3) used for the graphical visualisation of the isotope concept in Figure 2. However, it is worth noting that  $\Delta^{26}$ Mg<sub>wheat-rem. exch.</sub> determined in this field study remained constant throughout the growing stages of flowering and maturity, which conflicts with pot experiment results from Wang et al., (2020) who attributed different magnitudes of Mg isotope fractionation at different growing stages to a change in the Mg uptake strategy by switching between active and passive pathways. However, the disparity of plant-uptake related apparent Mg isotope fractionation factors when determined from pot experiments and field samples (Kimmig et al., 2018), or from mineral cultures and hydroponic systems (Bolou-Bi et al., 2010) is a known phenomenon. Thus, aiming at applying Mg stable isotopes as a new tool not only in agronomy but also in other ecosystems such as grasslands, tundra, and forests, requires a more comprehensive approach on the determination of  $\Delta^{26} Mg_{plant-rem.\ exch.}$  under field conditions and at multiple growing stages.

Moreover, to further substantiate these findings, future field studies should include root sampling. If done, three still unresolved challenges should be addressed. First, due to the strong intraplant translocation of Mg, both fine and coarse roots could carry different Mg isotope compositions that would remain unconsidered if root sampling is incomplete. Second, the conventional cleaning of roots prior to digestion with deionised water could include the risk of cell water extraction, as Tang et al (2016) used deionized water to extract intracellular Zn. Third, the presence of mycorrhiza introduces additional complexity for the in-field determination of plant uptake-related apparent Mg isotope fractionation factors.

#### 5.3. Isotope-derived Mg use efficiency and the effect of lime on the $\delta^{26}$ Mg<sub>exch.,i</sub> value

An assessment of the success of subsoil management requires not only yield measures but also nutrient use efficiency measures, here evaluated for Mg. A measure of the Mg use efficiency of crops at individual soil horizons was introduced in section 3.3.1 by means of fuptake, i (equation 8), which either serves as a non-isotope derived metric (e.g., as applied in the isotope concept for Figure 2), or which can be quantified solely from Mg isotopes, if the  $\delta^{26}$ Mg<sub>exch.,i</sub> value and  $\Delta^{26}$ Mg<sub>crop-rem, exch.,i</sub> can be determined from field samples. Consequently, the isotope-derived relative change in the Mg use efficiency at soil horizon i among the management and the control can be obtained from  $f_{\mathrm{uptake},i}^{\mathrm{management}} - f_{\mathrm{uptake},i}^{\mathrm{control}}$  (equation 12). Importantly, equation 12 only holds in quantitative terms, if external inputs like atmospheric deposition as well as soil improving (agricultural lime) and yieldincreasing substances (fertilizer), and any soil-plant processes beyond Mg uptake by crops affecting the exchangeable fraction of Mg in soil remain identical among the management and the control.  $f_{uptake,i}^{management} - f_{uptake,i}^{control} \text{ was calculated using } \Delta^{26} \text{Mg}_{\text{wheat-rem. exch.}} \text{ and } \Delta^{26} \text{Mg}_{\text{barley-rem. exch.}} \text{ (section 6.2) for } f_{uptake,i}^{management} - f_{uptake,i}^{control} \text{ was calculated using } \Delta^{26} \text{Mg}_{\text{wheat-rem. exch.}} \text{ and } \Delta^{26} \text{Mg}_{\text{barley-rem. exch.}} \text{ (section 6.2) for } f_{uptake,i}^{control} \text{ was calculated using } \Delta^{26} \text{Mg}_{\text{wheat-rem. exch.}} \text{ and } \Delta^{26} \text{Mg}_{\text{barley-rem. exch.}} \text{ (section 6.2) for } f_{uptake,i}^{control} \text{ was calculated using } \Delta^{26} \text{Mg}_{\text{wheat-rem. exch.}} \text{ and } \Delta^{26} \text{Mg}_{\text{barley-rem. exch.}} \text{ (section 6.2) for } f_{uptake,i}^{control} \text{ was calculated using } \Delta^{26} \text{Mg}_{\text{wheat-rem. exch.}} \text{ (section 6.2) for } f_{uptake,i}^{control} \text{ (sect$ DL plots and where the deep-rooting pre-crop lucerne was used. Figure 7 indicates that the Mg use efficiency apparently improved at most subsoil horizons by about 2% to 17%, which conflicts in two ways with the isotope concept. First, less Mg was taken up at greater depth with subsoil management. Second,  $f_{uptake,i}^{management} - f_{uptake,i}^{control}$  ranged from -1% to 3% for Alfisols (Supplementary Information 3) in the isotope concept that was applied to only two soil horizons. Given the rule of thumb that Mg isotope shifts and thus  $f_{\mathrm{uptake},i}^{\mathrm{management}} - f_{\mathrm{uptake},i}^{\mathrm{control}}$  are dampened with the contribution of more than two soil horizons to crop nutrition,  $f_{uptake,i}^{management} - f_{uptake,i}^{control}$  values beyond the above mentioned range indicate the presence of an additional controlling factor on the Mg isotope composition of the exchangeable fraction in soil that differs among the control and managed plots. It is worth noting that the depth distribution of  $f_{uptake,i}^{management} - f_{uptake,i}^{control}$  of the winter wheat and spring barley cultivation in 2018 correlate linearly (Figure 7,  $R^2$  = 0.94, not shown), so do, albeit less pronounced ( $R^2$  = 0.41, not shown) their cultivations in 2019 and 2020. That both pairs differ in shape from one another indeed suggests an additional controlling factor on the Mg isotope composition of the exchangeable fraction in soil. Such a potential factor may be the application of agricultural lime or any other Mg containing mineral fertilizer to the field that is – from a microscale perspective – heterogenous. Thus, the effect of agricultural lime is evaluated next.

Albeit incompletely documented, the application of Mg-carbonate containing fertilizer (CAN) and agricultural lime is conducted annually or every few years, respectively, to agricultural fields in the course of good management practices, as done at the field trials of this study. Whereas the application of about 30 g CAN m<sup>-2</sup> annually adds about 1.1 g Mg m<sup>-2</sup>, which is about  $\leq$  1% of  $I_{exch}^{Mg}$  and thus neglected hereafter, Mg addition through liming is substantial. For example, in 2015 (0.3 kg m<sup>-2</sup>) and 2016 (0.4 kg m<sup>-2</sup>) lime containing about 21 g Mg m<sup>-2</sup> with a  $\delta^{26}$ Mg<sub>lime</sub> value of -1.38% was added to the field trials of this study. This amount accounted for ~0.4% of  $I_{soil}^{Mg}$  but for as much as ~15% of  $I_{exch.}^{Mg}$ . Therefore, additions of Mg from lime were too low to affect the  $\delta^{26}$ Mg<sub>soil</sub> value (0.08 ± 0.10%, mean ± 2SD, N=83) but large enough to dominate the  $\delta^{26}$ Mg<sub>rem. exch.,i</sub> value (-1.27 ± 0.28‰, mean ± 2SD, N=83). Two lines of evidence support that lime exerts a strong control on the  $\delta^{26}$ Mg<sub>rem, exch.,i</sub> value. First, soil pH values range not only from 6.6 to 8.1, which are too high to be explained without frequent liming activities in a soil-plant system, but also moderately correlate with  $\delta^{26}Mg_{rem.\,exch.,i}$  values (R<sup>2</sup> ~ 0.48, not shown). Second, a strong negative correlation (R<sup>2</sup> ~0.72, not shown) between  $\delta^{26}$ Mg<sub>rem. exch.,i</sub> values and the Ca/Mg concentration ratio of the exchangeable soil fraction is indicative of carbonate contributions. However, the shallow bulge shaped depth profiles of  $\delta^{26}$ Mg<sub>rem. exch.,i</sub> values (Figure 5bc, e-g, i-k, m-o) differ from the unidirectional trend in depth profiles of  $\delta^{26}$ Mg<sub>exch.</sub> values in other studies, where lime was applied (e.g., Bolou-Bi et al., 2016; Wang et al., 2021). This discrepancy is attributed to a counteracting process operating at the field trials of this study, where Mg-carbonates are abundant at quantities of about 12.7 wt.% below 127 cm depth (Barej et al., 2014). Thus, Mgcarbonates may be dissolved at depth, relocated towards surface by upward moving soil solution and eventually end up in the soil exchange complex. The relocation of dissolved Mg may be triggered by  $evapotran spiration \ of \ crops \ or \ capillary \ rise. \ Returning \ to \ the \ contrasting \ f_{uptake,i}^{management} - f_{uptake,i}^{control}$ values among the isotope concept and the field trials of this study, this discrepancy is likely the result of the heterogenous application of lime onto soil followed by dissolution at the deposited soil patches below which it enters the soil exchange complex via preferential flow pathways along soil macro- and biopores. Thus, the heterogenous application at the surface translates into and even strengthens with depth, where the only minute Mg isotope shifts caused by Mg uptake by crops are likely overlayed by carbonate-derived Mg from CAN, agricultural lime or the field trials' *in situ* Mg-carbonates.

# 5.4. Criteria catalogue and future developments on the application of Mg stable isotopes in agronomy

Combining the Mg isotope concept with measured data from field trials enables the provision of a criteria catalogue that ensures the resolution of Mg isotope shifts in crops and the exchangeable fraction of Mg in soil among a control and a subsoil managed plot from the uncertainty of Mg isotope analyses. First, one of the most important criteria for the application of Mg stable isotopes in both a qualitative and quantitative sense, is the presence of a representative control. This control sets the limit for the correction of i) non-crop uptake-related Mg isotope fractionation (e.g., net formation of secondary solids), ii) solubilisation of Mg inputs (e.g., atmospheric dry deposition, SOM, soil minerals, organic and inorganic fertilizer, agricultural lime) and iii) Mg uptake by previous crop cultivations (e.g., crop and catch crop rotation). Second, the crop uptake-related apparent Mg isotope fractionation factor ( $\Delta^{26}$ Mg<sub>crop-rem. exch.</sub>) should be at the upper end of hitherto published apparent fractionation factors to attain maximum slopes of the lines shown in Figure 2a, d to maximize  $\Delta_{\mathrm{exch.i}}^{\mathrm{control-management}}$ and/or  $\Delta_{crop}^{control-management}$ . Considering  $\Delta^{26} Mg_{crop-rem.\, exch.}$  estimated from field trials in this study, winter wheat is better suited than spring barley to trace changes of the Mg uptake depth or differences in the Mg use efficiency (  $f_{uptake,i}^{management} - f_{uptake,i}^{control}$ ) caused by subsoil management. Third, a large Mg uptake flux ( $U_{net}^{Mg}$ ) should be matched by a low inventory of Mg in the exchangeable fraction in soil  $(I_{\mathrm{exch.}}^{\mathrm{Mg}})$  to allow maximum differences in  $f_{\mathrm{uptake,i}}$  among soil samples collected from managed and nonmanaged plots, because, apart from  $\Delta^{26}$ Mg<sub>crop-rem. exch.</sub>,  $f_{uptake}$  dictates the ordinate position in Figure 2a, d. This criterion is best achieved on soils with a low cation-exchange capacity (e.g., sandy soils, tropical soils) and by the cultivation of crops with high  $U_{net}^{Mg}$ . Fourth, if the evaluation of the success of subsoil management is desired only in a qualitative sense, the incorporation of organic matter or any other quickly decomposing or dissolving material at depth with a different Mg isotope composition than the surrounding soil and a Mg concentration at a natural abundance level is recommended.

This criteria catalogue should be understood as an initial step towards the implementation of a new geochemical routine in agronomy and soil/plant sciences. The practical realisation still poses challenges that need to be solved such as the reduction of the number of samples and analytical effort. For example, the exchangeable fraction best reflects any effect of isotope fractionation caused by the crops' response to subsoil management but requires not only invasive soil sampling but also a high depth resolution, resulting in many samples. In contrast, whole crop sampling is easy, quick, and minimally invasive, but due to the depth integrative character of Mg uptake the magnitude of isotope

fractionation is lowest among the soil-plant compartments and seems to depend on crop species (section 6.2). Thus, to deduce the same information on changes in the crops' Mg uptake depth and their Mg use efficiency from a single crop organ as from the whole crop or the exchangeable fraction of a given soil horizon, species-dependent Mg isotope fractionation factors and a systemic understanding of Mg isotope fractionation during intra-plant translocation are needed along with algorithms, developed from sophisticated numerical models, to correct for these effects. In addition, analytical progress is required to improve the long-term external precision of Mg isotope analyses, which would even resolve the minute Mg isotope shifts caused by the crop's response to subsoil management in soils of high inventories of exchangeable Mg. Thus, future studies of interdisciplinary approach are required to develop geochemical methods as routine tools in agronomy, and soil/plant sciences.

#### 6. Conclusions

As a representative for metal(loid) isotope systems, Mg stable isotopes have been suggested as a new tool for the evaluation of subsoil management. Two lines of evidence supported this new application. First, an isotope concept demonstrated that the magnitude of shifts in the Mg isotope composition of the exchangeable fraction of Mg in any soil horizon and of bulk whole crops could be resolved from the uncertainty of Mg isotope analyses if i) the crop uptake-related Mg isotope fractionation factor is large (e.g., for wheat), ii) a high Mg uptake flux of crop plants (e.g., sugar beets) is matched by low Mg supply from the exchangeable fraction (e.g., in sandy soils, tropical soils), and iii) subsoil management causes a considerable deepening of the rooting system (e.g., flipping the topsoil root cluster below 30 cm depth). Second, this isotope concept was positively tested for Alfisols (represented by Luvisols in this study) on field trials where subsoil management was conducted. This positive test was manifested by distinct  $\delta^{26}$ Mg values of bulk whole crops sampled from a meliorated strip and next to it. However, the field study also showed that the application of Mg stable isotopes as subsoil management evaluation tool has limitations. For example, when agricultural lime or fertilizer containing Mg-carbonates are involved in agricultural practices, caution must be taken when calculating differences in the Mg use efficiency among the control and subsoil managed plots solely from Mg stable isotopes. Similarly, when subsoil management involves the incorporation of compost with additional Mg of distinct isotope composition than the surrounding soil, Mg isotopes should be used in a qualitative sense only, e.g., in an isotope label like approach. However, altogether Mg stable isotopes are indeed a novel tool for subsoil management evaluation, as they trace and quantify changes in the Mg uptake depth and Mg use efficiency, respectively.

#### 7. Acknowledgements

The authors are grateful to the German Federal Ministry of Education and Research (BMBF) for funding the project "BonaRes (Module A): Sustainable Subsoil Management – Soil³-II; subproject C" (grant number 031B0515C) and to the staff of the Campus Klein-Altendorf, particularly to Oliver Schmittmann (University of Bonn), for installing the central field experiments. For analytical support, the authors are thankful to Volker Nischwitz, Nadine Wettengl, Sabrina Tückhardt and Ulrike Seeling from the Central Institute of Engineering, Electronics and Analytics (ZEA-3) at Forschungszentrum Jülich GmbH. The authors also acknowledge analytical support from the trainees Anna-Lena Lohe, Antonio Voss, Jan-Philipp Treitz and the student assistants Claudia Tahiraj and Ying Xing. Finally, the authors are grateful to the constructive reviews by Sara R. Kimmig and one anonymous reviewer that helped to improve the manuscript, as well as to Michael E. Böttcher for manuscript handling.

#### 8. Competing interest

The authors declare that they have no conflict of interest.

#### 9. Appendix

#### **Appendix A: Supplementary Material**

Supplementary information to this article can be found online at https://doi.org/....

#### **Appendix B: Doping experiments**

The standard-sample-standard bracketing method is applied in stable isotope analyses to account for slight, unidirectional, and predictable changes in the mass bias during a standard-sample-standard sequence. However, the presence of matrix elements in the sample and its lack in the standard can change the proportion of ion transmission efficiencies of <sup>24</sup>Mg, <sup>25</sup>Mg and <sup>26</sup>Mg during ion extraction that results in shifts in the mass bias. To test for shifts in the mass bias, and hence in the Mg isotope composition, doping experiments are required. To date the effects of Ca and Fe impurities on the Mg isotope composition were thoroughly tested (An et al., 2014; Bao et al., 2019; Choi et al., 2012; Galy et al., 2001; Hu and Teng, 2019; Li et al., 2012; Teng and Yang, 2014; Wombacher et al., 2009). Also, the effects of Co and Cu on the Mg isotope composition were tested to maximum impurity levels of as low as 2% for Co (Wang et al., 2011) and as high as 600% for Cu (Bao et al., 2019). Results of previous doping experiments were considerably variable and were attributed to different instruments, instrumental settings, and Mg concentrations (Teng and Yang, 2014). Thus, doping experiments for Ca, Cu, Fe, and Zn were repeated, and extended to higher levels of Co to assess the effect of isobaric

interferences, for example, of <sup>48</sup>Ca<sup>2+</sup> on <sup>24</sup>Mg<sup>+</sup>, and potential matrix effects of Co, Cu, Fe, Zn on the Mg isotope composition at the same instrumental settings as used for field samples in this study.

Results are summarized in Figure A1. No matrix effects were found for Cu and Zn to impurity levels of up to 60% and for Co to up to 75%. Yet, substantial effects were found for Ca impurities >5% and Fe impurities >20%. These results are both in line and contrary to previous findings. For example, for Ca the same abrupt shift in the mass bias were found as demonstrated by Wombacher et al., (2009) (Axiom, wet plasma, 600 – 2500 ng g<sup>-1</sup> Mg). Also, the Mg isotope composition is shifted towards more positive values at Ca impurities >5% (Figure A1a) as in Galy et al., (2001) (Nu Instruments, dry plasma, 500 – 1500 ng g<sup>-1</sup> Mg). In contrast, no effects of Ca impurities on the Mg isotope composition were found in Teng and Yang (2014) (Nu plasma, dry plasma, 200 ng g<sup>-1</sup> Mg) for Ca levels up to 30%, in An et al., (2014) (Neptune, wet plasma, 500 – 2000 ng g<sup>-1</sup> Mg) and in Hu and Teng (2019) (Nu plasma, wet plasma, 150 ng g<sup>-1</sup> Mg) for Ca levels up to 50% and in Choi et al., (2012) (Neptune, cool plasma, 90V per ppm Mg) for Ca levels to up to 100%. Also, An et al., (2014) and Hu and Teng (2019) found the opposite direction in the shift of the Mg isotope composition as found in this study and in Galy et al., (2001).

With respect to Fe, Mg isotope analyses were found to be more tolerant to Fe impurities when measured in wet plasma mode – as demonstrated, e.g., by Hu and Teng (2019) – than in dry plasma mode – as demonstrated by e.g., Teng and Yang (2014). However, Fe doping experiments in wet plasma mode of this study revealed a substantial shift towards more positive  $\delta^{26}$ Mg values at Fe impurities >40% (Figure A1g) at which Hu and Teng (2019) found no effect. This difference was attributed to different Mg concentrations of the analysed solutions, as impurity experiments of this study were performed at 600 ng g<sup>-1</sup> Mg but Hu and Teng (2019) have chosen 150 ng g<sup>-1</sup> Mg. Consequently, the higher amounts of Fe and Mg and the higher ion density in the ion beam may have caused shifts in  $\delta^{26}$ Mg values at lower Fe:Mg ratios in this study than found in Hu and Teng (2019). Similarly, the higher ion density may have altered the ion transmission efficiency during ion extraction in the opposite direction as in Teng and Yang (2014) for Fe, or Hu and Teng (2019) for Ca, explaining why  $\delta^{26}$ Mg values dropped with increasing amounts of Fe or Ca in the respective earlier studies but increased in this study.

#### Appendix C: Does incomplete sample digestion affect $\delta^{26}$ Mg values?

Given that the self-made, low particulate clean laboratory used in this study did not allow the evaporation of concentrated hydrofluoric acid (HF), a full digestion of silicate minerals was not possible. Hence, a critical eye on any potential effect of this practice is casted to the Mg isotope data of this study. Figure 3b-d revealed a slight shift of  $\delta^{26}$ Mg values measured on standard reference materials (SRM) to previously published  $\delta^{26}$ Mg values towards more positive  $\delta^{26}$ Mg values. Even

though this shift is negligible within uncertainties, it is systematic and may be caused by incomplete sample digestion before loading the sample on the cation-exchange resin. However, the non-application of concentrated HF had, if any, only a minor effect on  $\delta^{26}$ Mg values of the sample types processed in this study as demonstrated by the comparison of  $\delta^{26}$ Mg values of HF treated NIST SRM 2709a San Joaquin soil (literature values) with our data (microwave digestion without HF) in Figure 3d.

#### 10. Research Data

Research Data associated with this article can be accessed at GFZ Data Services under the reference Uhlig (2022). Tables S1–S5 include the dataset discussed in this publication along with further background data.

#### 11. References

- An, Y., Wu, F., Xiang, Y., Nan, X., Yu, X., Yang, J., Yu, H., Xie, L., Huang, F., 2014. High-precision Mg isotope analyses of low-Mg rocks by MC-ICP-MS. Chem. Geol. 390, 9–21. https://doi.org/10.1016/j.chemgeo.2014.09.014
- Arunachalam, J., Emons, H., Krasnodebska, B., Mohl, C., 1996. Sequential extraction studies on homogenized forest soil samples. Sci. Total Environ. 181, 147–159. https://doi.org/10.1016/0048-9697(95)05005-1
- Bao, Z., Huang, K., Huang, T., Shen, B., Zong, C., Chen, K., Yuan, H., 2019. Precise magnesium isotope analyses of high-K and low-Mg rocks by MC-ICP-MS. J. Anal. At. Spectrom. 34, 940–953. https://doi.org/10.1039/c9ja00002j
- Barej, J.A.M., Pätzold, S., Perkons, U., Amelung, W., 2014. Phosphorus fractions in bulk subsoil and its biopore systems. Eur. J. Soil Sci. 65, 553–561. https://doi.org/10.1111/ejss.12124
- Beißmann, J., 2021. The ability of arbuscular mycorrhizal fungi to transport iron from poorly soluble compounds into spring barley (Hordeum vulgare). RWTH Aachen.
- Bélanger, N., Holmden, C., 2010. Influence of landscape on the apportionment of Ca nutrition in a Boreal Shield forest of Saskatchewan (Canada) using 87Sr/86Sr as a tracer. Can. J. Soil Sci. 90, 267–288. https://doi.org/10.4141/cjss09079
- Benker, M., Röhling, D., Schmid, M., 2016. Ratgeber Pflanzenbau und Pflanzenschutz. Landwirtschaftskammer Nordrhein-Westfalen.
- Black, J.R., Epstein, E., Rains, W.D., Yin, Q.Z., Casey, W.H., 2008. Magnesium-isotope fractionation during plant growth. Environ. Sci. Technol. 42, 7831–7836. https://doi.org/10.1021/es8012722
- Black, J.R., Yin, Q. zhu, Casey, W.H., 2006. An experimental study of magnesium-isotope fractionation in chlorophyll-a photosynthesis. Geochim. Cosmochim. Acta 70, 4072–4079. https://doi.org/10.1016/j.gca.2006.06.010
- Blanco-Canqui, H., Wienhold, B.J., Jin, V.L., Schmer, M.R., Kibet, L.C., 2017. Long-term tillage impact on soil hydraulic properties. Soil Tillage Res. 170, 38–42. https://doi.org/10.1016/j.still.2017.03.001
- Bohlin, M.S., Misra, S., Lloyd, N., Elderfield, H., Bickle, M.J., 2018. High-precision determination of lithium and magnesium isotopes utilising single column separation and multi-collector

- inductively coupled plasma mass spectrometry. Rapid Commun. Mass Spectrom. 32, 93–104. https://doi.org/10.1002/rcm.8020
- Bolou-Bi, B.E., Dambrine, E., Angeli, N., Pollier, B., Nys, C., Guerold, F., Legout, A., 2016. Magnesium Isotope Variations to Trace Liming Input to Terrestrial Ecosystems. J. Environ. Qual. 45, 276–284.
- Bolou-Bi, E.B., Poszwa, A., Leyval, C., Vigier, N., 2010. Experimental determination of magnesium isotope fractionation during higher plant growth. Geochim. Cosmochim. Acta 74, 2523–2537. https://doi.org/10.1016/j.gca.2010.02.010
- Bolou-Bi, E.B., Vigier, N., Poszwa, A., Boudot, J.P., Dambrine, E., 2012. Effects of biogeochemical processes on magnesium isotope variations in a forested catchment in the Vosges Mountains (France). Geochim. Cosmochim. Acta 87, 341–355. https://doi.org/10.1016/j.gca.2012.04.005
- Bullen, T., Chadwick, O., 2016. Ca, Sr and Ba stable isotopes reveal the fate of soil nutrients along a tropical climosequence in Hawaii. Chem. Geol. 422, 25–45. https://doi.org/10.1016/j.chemgeo.2015.12.008
- Bullen, T.D., 2014. Metal stable isotopes in weathering and hydrology: Chapter 10, in: US Geological Survey. pp. 329–359.
- Cai, D., Henehan, M.J., Uhlig, D., von Blanckenburg, F., 2022. Mg isotope composition of runoff is buffered by the regolith exchangeable pool. Geochim. Cosmochim. Acta 99–114. https://doi.org/https://doi.org/10.1016/j.gca.2022.01.011
- Canadell, J., Jackson, R.B., Ehleringer, J.B., Mooney, H.A., Sala, O.E., Schulze, E.-D., 1996. Maximum rooting depth of vegetation types at the global scale. Oecologia 108, 583–595. https://doi.org/10.1007/BF00329030
- Chapin, S.F., Matson, P.A., Vitousek, P.M., 2012. Principles of terrestrial ecosystem ecology, Second. ed, Principles of Terrestrial Ecosystem Ecology. Springer New York Dordrecht Heidelberg London. https://doi.org/10.1007/978-1-4419-9504-9
- Choi, M.S., Ryu, J.-S., Lee, S.-W., Shin, H.S., Lee, K.-S., 2012. A revisited method for Mg purification and isotope analysis using cool-plasma MC-ICP-MS. J. Anal. At. Spectrom. 27, 1955. https://doi.org/10.1039/c2ja30191a
- Coble, A.A., Hart, S.C., Ketterer, M.E., Newman, G.S., Kowler, A.L., 2015. Strontium source and depth of uptake shifts with substrate age in semiarid ecosystems. J. Geophys. Res. Biogeosciences 120, 1069–1077. https://doi.org/10.1002/2015JG002992.Received
- Fahad, Z.A., Bolou-Bi, E.B., Köhler, S.J., Finlay, R.D., Mahmood, S., 2016. Fractionation and assimilation of Mg isotopes by fungi is species dependent. Environ. Microbiol. Rep. 8, 956–965. https://doi.org/10.1111/1758-2229.12459
- Gaiser, T., Perkons, U., Küpper, P.M., Puschmann, D.U., Peth, S., Kautz, T., Pfeifer, J., Ewert, F., Horn, R., Köpke, U., 2012. Evidence of improved water uptake from subsoil by spring wheat following lucerne in a temperate humid climate. F. Crop. Res. 126, 56–62. https://doi.org/10.1016/j.fcr.2011.09.019
- Galy, A., Belshaw, N.S., Halicz, L., O'Nions, R.K., 2001. High-precision measurement of magnesium isotopes by multiple- collector inductively coupled plasma mass spectrometry. Int. J. Mass Spectrom. 208, 89–98. https://doi.org/10.1016/S1387-3806(01)00380-3
- Gao, T., Ke, S., Wang, S.J., Li, F., Liu, C., Lei, J., Liao, C., Wu, F., 2018. Contrasting Mg isotopic compositions between Fe-Mn nodules and surrounding soils: Accumulation of light Mg isotopes by Mg-depleted clay minerals and Fe oxides. Geochim. Cosmochim. Acta 237, 205–222.

- https://doi.org/10.1016/j.gca.2018.06.028
- Geological and Environmental Reference Materials (GeoReM), Max-Planck-Gesellschaft, http://georem.mpch-mainz.gwdg.de (accessed 22. January 2021)
- Hindshaw, R.S., Tosca, R., Tosca, N.J., Tipper, E.T., 2020. Experimental constraints on Mg isotope fractionation during clay formation: Implications for the global biogeochemical cycle of Mg. Earth Planet. Sci. Lett. 531, 115980. https://doi.org/10.1016/j.epsl.2019.115980
- Hinzmann, M., Ittner, S., Kiresiewa, Z., Gerdes, H., 2021. An Acceptance Analysis of Subsoil Amelioration Amongst Agricultural Actors in Two Regions in Germany. Front. Agron. 3, 1–14. https://doi.org/10.3389/fagro.2021.660593
- Hu, Y., Teng, F.-Z., 2019. Optimization of analytical conditions for precise and accurate isotope analyses of Li, Mg, Fe, Cu, and Zn by MC-ICPMS. J. Anal. At. Spectrom. 1–9. https://doi.org/10.1039/C8JA00335A
- IPCC, 2019. Summary for Policymakers, in: Shukla, P.R., Skea, J., Buendia, E.C., Masson-Delmotte, V., Pörtner, H.-O., Roberts, D.C., Zhai, P., Slade, R., Connors, S., Diemen, R. van, Ferrat, M., Haughey, E., Luz, S., Neogi, S., Pathak, M., Petzold, J., Pereira, J.P., Vyas, P., Huntley, E., Kissick, K. (Eds.), Climate Change and Land: An IPCC Special Report on Climate Change, Desertification, Land Degradation, Sustainable Land Management, Food Security, and Greenhouse Gas Fluxes in Terrestrial Ecosystems. pp. 1–41. https://doi.org/10.1002/9781118786352.wbieg0538
- IUSS Working Group WRB. 2015, n.d. World reference base for soil resources 2014, update 2015, International soil classification system for naming soils and creating legends for soil maps. World Soil Resources Report 106. Rome, Italy: Food and Agriculture Organization of the United Nations. https://doi.org/10.1017/S0014479706394902
- Jackson, R.B., Canadell, J., Ehleringer, J.R., Mooney, H.A., Sala, O.E., Schulze, E.D., 1996. A global analysis of root distributions for terrestrial biomes. Oecologia 108, 389–411. https://doi.org/10.1007/BF00333714
- Jakobs, I., Schmittmann, O., Athmann, M., Kautz, T., Lammers, P.S., 2019. Cereal Response to Deep Tillage and Incorporated Organic Fertilizer. Agronomy 9, 1–16. https://doi.org/doi:10.3390/agronomy9060296
- Jobbágy, E.G., Jackson, R.B., 2004. The uplift of soil nutrients by plants: Biogeochemical consequences across scales. Ecology 85, 2380–2389. https://doi.org/10.1890/03-0245
- Jochum, K.P., Nohl, U., Herwig, K., Lammel, E., Stoll, B., Hofmann, A.W., 2005. GeoReM: A New Geochemical Database for Reference Materials and Isotopic Standards. Geostand. Geoanalytical Res. 29, 333–338. https://doi.org/10.1111/j.1751-908X.2005.tb00904.x
- Kautz, T., Amelung, W., Ewert, F., Gaiser, T., Horn, R., Jahn, R., Javaux, M., Kemna, A., Kuzyakov, Y., Munch, J.C., Pätzold, S., Peth, S., Scherer, H.W., Schloter, M., Schneider, H., Vanderborght, J., Vetterlein, D., Walter, A., Wiesenberg, G.L.B., Köpke, U., 2013. Nutrient acquisition from arable subsoils in temperate climates: A review. Soil Biol. Biochem. https://doi.org/10.1016/j.soilbio.2012.09.014
- Kimmig, S.R., Holmden, C., Bélanger, N., 2018. Biogeochemical cycling of Mg and its isotopes in a sugar maple forest in Québec. Geochim. Cosmochim. Acta 230, 60–82. https://doi.org/10.1016/j.gca.2018.03.020
- Kirkegaard, J.A., Lilley, J.M., Howe, G.N., Graham, J.M., 2007. Impact of subsoil water use on wheat yield. Aust. J. Agric. Res. 58, 303–315. https://doi.org/10.1071/AR06285
- Li, M.Y.H., Teng, F.Z., Zhou, M.F., 2021. Phyllosilicate controls on magnesium isotopic fractionation

- during weathering of granites: Implications for continental weathering and riverine system. Earth Planet. Sci. Lett. 553, 116613. https://doi.org/10.1016/j.epsl.2020.116613
- Li, W., Beard, B.L., Li, C., Johnson, C.M., 2014. Magnesium isotope fractionation between brucite [Mg(OH)2] and Mg aqueous species: Implications for silicate weathering and biogeochemical processes. Earth Planet. Sci. Lett. 394, 82–93. https://doi.org/10.1016/j.epsl.2014.03.022
- Li, W., Chakraborty, S., Beard, B.L., Romanek, C.S., Johnson, C.M., 2012. Magnesium isotope fractionation during precipitation of inorganic calcite under laboratory conditions. Earth Planet. Sci. Lett. 333–334, 304–316. https://doi.org/10.1016/j.epsl.2012.04.010
- Liu, X.M., Teng, F.Z., Rudnick, R.L., McDonough, W.F., Cummings, M.L., 2014. Massive magnesium depletion and isotope fractionation in weathered basalts. Geochim. Cosmochim. Acta 135, 336–349. https://doi.org/10.1016/j.gca.2014.03.028
- Ma, L., Teng, F.Z., Jin, L., Ke, S., Yang, W., Gu, H.O., Brantley, S.L., 2015. Magnesium isotope fractionation during shale weathering in the Shale Hills Critical Zone Observatory: Accumulation of light Mg isotopes in soils by clay mineral transformation. Chem. Geol. 397, 37–50. https://doi.org/10.1016/j.chemgeo.2015.01.010
- Maher, K., Johnson, N.C., Jackson, A., Lammers, L.N., Torchinsky, A.B., Weaver, K.L., Bird, D.K., Brown, G.E., 2016. A spatially resolved surface kinetic model for forsterite dissolution. Geochim. Cosmochim. Acta 174, 313–334. https://doi.org/10.1016/j.gca.2015.11.019
- Marks, M.J., Soane, G.C., 1987. Crop and soil response to subsoil loosening, deep incorporation of phosphorus and potassium fertilizer and subsequent soil management on a range of soil types. Part 1: Response of arable crops. SOIL USE Manag. 3, 115–123.
- Marschner, P., 2011. Marschner's Mineral Nutrition of Higher Plants. https://doi.org/10.1016/B978-0-12-384905-2.00001-7
- Mavromatis, V., Gautier, Q., Bosc, O., Schott, J., 2013. Kinetics of Mg partition and Mg stable isotope fractionation during its incorporation in calcite. Geochim. Cosmochim. Acta 114, 188–203. https://doi.org/10.1016/j.gca.2013.03.024
- Mavromatis, V., Prokushkin, A.S., Pokrovsky, O.S., Viers, J., Korets, M.A., 2014. Magnesium isotopes in permafrost-dominated Central Siberian larch forest watersheds. Geochim. Cosmochim. Acta 147, 76–89. https://doi.org/10.1016/j.gca.2014.10.009
- McCulley, R.L., Jobbágy, E.G., Pockman, W.T., Jackson, R.B., 2004. Nutrient uptake as a contributing explanation for deep rooting in arid and semi-arid ecosystems. Oecologia 141, 620–628. https://doi.org/10.1007/s00442-004-1687-z
- Moynier, F., Fujii, T., 2017a. Theoretical isotopic fractionation of magnesium between chlorophylls. Sci. Rep. 7, 1–6. https://doi.org/10.1038/s41598-017-07305-6
- Moynier, F., Fujii, T., 2017b. Calcium isotope fractionation between aqueous compounds relevant to low-temperature geochemistry, biology and medicine. Sci. Rep. 7, 1–7. https://doi.org/10.1038/srep44255
- Moynier, F., Fujii, T., Wang, K., Foriel, J., 2013. Ab initio calculations of the Fe(II) and Fe(III) isotopic effects in citrates, nicotianamine, and phytosiderophore, and new Fe isotopic measurements in higher plants. Comptes Rendus Geosci. 345, 230–240. https://doi.org/10.1016/j.crte.2013.05.003
- Novak, M., Farkas, J., Kram, P., Hruska, J., Stepanova, M., Veselovsky, F., Curik, J., Andronikov, A. V., Sebek, O., Simecek, M., Fottova, D., Bohdalkova, L., Prechova, E., Koubova, M., Vitkova, H., 2020a. Controls on δ26Mg variability in three Central European headwater catchments

- characterized by contrasting bedrock chemistry and contrasting inputs of atmospheric pollutants. PLoS One 15, e0242915. https://doi.org/10.1371/journal.pone.0242915
- Novak, M., Holmden, C., Farkas, J., Kram, P., Hruska, J., Curik, J., Veselovsky, F., Stepanova, M., Kochergina, Y. V, Erban, V., Andronikov, A., Sebek, O., Koubova, M., Bohdalkova, L., 2020b. Magnesium and calcium isotope systematics in a headwater catchment underlain by amphibolite: Constraints on Mg Ca biogeochemistry in an atmospherically polluted but well-buffered spruce ecosystem (Czech Republic, Central Europe). Catena 193, 104637. https://doi.org/10.1016/j.catena.2020.104637
- Odlare, M., Pell, M., Svensson, K., 2008. Changes in soil chemical and microbiological properties during 4 years of application of various organic residues. Waste Manag. 28, 1246–1253. https://doi.org/10.1016/j.wasman.2007.06.005
- Oelkers, E.H., Berninger, U.N., Pérez-Fernàndez, A., Chmeleff, J., Mavromatis, V., 2018. The temporal evolution of magnesium isotope fractionation during hydromagnesite dissolution, precipitation, and at equilibrium. Geochim. Cosmochim. Acta 226, 36–49. https://doi.org/10.1016/j.gca.2017.11.004
- Olesen, J.E., Munkholm, L.J., 2007. Subsoil loosening in a crop rotation for organic farming eliminated plough pan with mixed effects on crop yield. Soil Tillage Res. 94, 376–385. https://doi.org/10.1016/j.still.2006.08.015
- Opfergelt, S., Burton, K.W., Georg, R.B., West, A.J., Guicharnaud, R.A., Sigfusson, B., Siebert, C., Gislason, S.R., Halliday, A.N., 2014. Magnesium retention on the soil exchange complex controlling Mg isotope variations in soils, soil solutions and vegetation in volcanic soils, Iceland. Geochim. Cosmochim. Acta 125, 110–130. https://doi.org/10.1016/j.gca.2013.09.036
- Opfergelt, S., Georg, R.B., Delvaux, B., Cabidoche, Y.M., Burton, K.W., Halliday, A.N., 2012. Mechanisms of magnesium isotope fractionation in volcanic soil weathering sequences, Guadeloupe. Earth Planet. Sci. Lett. 341–344, 176–185. https://doi.org/10.1016/j.chemgeo.2012.07.032
- Pearce, C.R., Saldi, G.D., Schott, J., Oelkers, E.H., 2012. Isotopic fractionation during congruent dissolution, precipitation and at equilibrium: Evidence from Mg isotopes. Geochim. Cosmochim. Acta 92, 170–183. https://doi.org/10.1016/j.gca.2012.05.045
- Pogge von Strandmann, P.A.E., Burton, K.W., James, R.H., van Calsteren, P., Gislason, S.R., Sigfússon, B., 2008. The influence of weathering processes on riverine magnesium isotopes in a basaltic terrain. Earth Planet. Sci. Lett. 276, 187–197. https://doi.org/10.1016/j.epsl.2008.09.020
- Pokharel, R., Gerrits, R., Schuessler, J.A., Floor, G.H., Gorbushina, A.A., Von Blanckenburg, F., 2017. Mg Isotope Fractionation during Uptake by a Rock-Inhabiting, Model Microcolonial Fungus Knufia petricola at Acidic and Neutral pH. Environ. Sci. Technol. 51, 9691–9699. https://doi.org/10.1021/acs.est.7b01798
- Pokharel, R., Gerrits, R., Schuessler, J.A., Frings, P.J., Sobotka, R., Gorbushina, A.A., Von Blanckenburg, F., 2018. Magnesium Stable Isotope Fractionation on a Cellular Level Explored by Cyanobacteria and Black Fungi with Implications for Higher Plants. Environ. Sci. Technol. 52, 12216–12224. https://doi.org/10.1021/acs.est.8b02238
- Pokharel, R., Gerrits, R., Schuessler, J.A., von Blanckenburg, F., 2019. Mechanisms of olivine dissolution by rock-inhabiting fungi explored using magnesium stable isotopes. Chem. Geol. 525, 18–27. https://doi.org/10.1016/j.chemgeo.2019.07.001
- Ra, K., Kitagawa, H., 2007. Magnesium isotope analysis of different chlorophyll forms in marine phytoplankton using multi-collector ICP-MS. J. Anal. At. Spectrom. 22, 817. https://doi.org/10.1039/b701213f

- Ra, K., Kitagawa, H., Shiraiwa, Y., 2010. Mg isotopes in chlorophyll-a and coccoliths of cultured coccolithophores (Emiliania huxleyi) by MC-ICP-MS. Mar. Chem. 122, 130–137. https://doi.org/10.1016/j.marchem.2010.07.004
- Ryu, J.S., Jacobson, A.D., Holmden, C., Lundstrom, C., Zhang, Z., 2011. The major ion, δ44/40Ca, δ44/42Ca, and δ26/24Mg geochemistry of granite weathering at pH=1 and T=25°C: Power-law processes and the relative reactivity of minerals. Geochim. Cosmochim. Acta 75, 6004–6026. https://doi.org/10.1016/j.gca.2011.07.025
- Ryu, J.S., Vigier, N., Decarreau, A., Lee, S.W., Lee, K.S., Song, H., Petit, S., 2016. Experimental investigation of Mg isotope fractionation during mineral dissolution and clay formation. Chem. Geol. 445, 135–145. https://doi.org/10.1016/j.chemgeo.2016.02.006
- Saenger, C., Wang, Z., 2014. Magnesium isotope fractionation in biogenic and abiogenic carbonates: Implications for paleoenvironmental proxies. Quat. Sci. Rev. 90, 1–21. https://doi.org/10.1016/j.quascirev.2014.01.014
- Schmitt, A.D., Vigier, N., Lemarchand, D., Millot, R., Stille, P., Chabaux, F., 2012. Processes controlling the stable isotope compositions of Li, B, Mg and Ca in plants, soils and waters: A review. Comptes Rendus Geosci. https://doi.org/10.1016/j.crte.2012.10.002
- Schmittmann, O., Christ, A., Lammers, P.S., 2021. Subsoil melioration with organic material—principle, technology and yield effects. Agronomy 11. https://doi.org/10.3390/agronomy11101970
- Schneider, F., Amelung, W., Don, A., 2021. Origin of carbon in agricultural soil profiles deduced from depth gradients of C:N ratios, carbon fractions,  $\delta$ 13C and  $\delta$ 15N values. Plant Soil 460, 123–148. https://doi.org/10.1007/s11104-020-04769-w
- Schneider, F., Don, A., 2019a. Root-restricting layers in German agricultural soils. Part I: extent and cause. Plant Soil 433–451. https://doi.org/10.1007/s11104-019-04185-9
- Schneider, F., Don, A., 2019b. Root-restricting layers in German agricultural soils. Part II: Adaptation and melioration strategies. Plant Soil 419–432. https://doi.org/10.1007/s11104-019-04185-9
- Schott, J., Mavromatis, V., Fujii, T., Pearce, C.R., Oelkers, E.H., 2016. The control of carbonate mineral Mg isotope composition by aqueous speciation: Theoretical and experimental modeling. Chem. Geol. 445, 120–134. https://doi.org/10.1016/j.chemgeo.2016.03.011
- Schuessler, J.A., Kämpf, H., Koch, U., Alawi, M., 2016. Earthquake impact on iron isotope signatures recorded in mineral spring water Suppl. J. Geophys. Res. Solid Earth 121, 8548–8568. https://doi.org/10.1002/2016JB013408
- Schuessler, J.A., von Blanckenburg, F., Bouchez, J., Uhlig, D., Hewawasam, T., 2018. Nutrient cycling in a tropical montane rainforest under a supply-limited weathering regime traced by elemental mass balances and Mg stable isotopes. Chem. Geol. 497, 74–87. https://doi.org/10.1016/j.chemgeo.2018.08.024
- Soil Survey Staff, 1999. Soil Taxonomy A Basic System of Soil Classification for Making and Interpreting Soil Surveys, 2nd ed.
- Spohn, M., Aburto, F., Ehlers, T.A., Farwig, N., Frings, P.J., Hartmann, H., Hoffmann, T., Larsen, A., Oelmann, Y., 2021. Terrestrial ecosystems buffer inputs through storage and recycling of elements. Biogeochemistry 0123456789. https://doi.org/10.1007/s10533-021-00848-x
- Tang, Y.T., Cloquet, C., Deng, T.H.B., Sterckeman, T., Echevarria, G., Yang, W.J., Morel, J.L., Qiu, R.L., 2016. Zinc Isotope Fractionation in the Hyperaccumulator Noccaea caerulescens and the Nonaccumulating Plant Thlaspi arvense at Low and High Zn Supply. Environ. Sci. Technol. 50,

- 8020-8027. https://doi.org/10.1021/acs.est.6b00167
- Teng, F.-Z., 2017. Magnesium Isotope Geochemistry. Rev. Mineral. Geochemistry 82, 219–287. https://doi.org/10.2138/rmg.2017.82.7
- Teng, F.Z., Li, W.Y., Ke, S., Marty, B., Dauphas, N., Huang, S., Wu, F.Y., Pourmand, A., 2010a. Magnesium isotopic composition of the Earth and chondrites. Geochim. Cosmochim. Acta 74, 4150–4166. https://doi.org/10.1016/j.gca.2010.04.019
- Teng, F.Z., Li, W.Y., Rudnick, R.L., Gardner, L.R., 2010b. Contrasting lithium and magnesium isotope fractionation during continental weathering. Earth Planet. Sci. Lett. 300, 63–71. https://doi.org/10.1016/j.epsl.2010.09.036
- Teng, F.Z., Yang, W., 2014. Comparison of factors affecting the accuracy of high-precision magnesium isotope analysis by multi-collector inductively coupled plasma mass spectrometry. Rapid Commun. Mass Spectrom. 28, 19–24. https://doi.org/10.1002/rcm.6752
- Tipper, E.T., 2022. Magnesium isotopes, in: Elements in Geochemical Tracers in Earth Sciences. Cambridge University Press, pp. 1–25. https://doi.org/10.1017/9781108991698
- Tipper, E.T., Calmels, D., Gaillardet, J., Louvat, P., Capmas, F., Dubacq, B., 2012. Positive correlation between Li and Mg isotope ratios in the river waters of the Mackenzie Basin challenges the interpretation of apparent isotopic fractionation during weathering. Earth Planet. Sci. Lett. 333–334, 35–45. https://doi.org/10.1016/j.epsl.2012.04.023
- Tipper, E.T., Gaillardet, J., Louvat, P., Capmas, F., White, A.F., 2010. Mg isotope constraints on soil pore-fluid chemistry: Evidence from Santa Cruz, California. Geochim. Cosmochim. Acta 74, 3883–3896. https://doi.org/10.1016/j.gca.2010.04.021
- Uhlig, D., Amelung, W., Von Blanckenburg, F., 2020. Mineral Nutrients Sourced in Deep Regolith Sustain Long-Term Nutrition of Mountainous Temperate Forest Ecosystems. Global Biogeochem. Cycles 34, 1–21. https://doi.org/10.1029/2019GB006513
- Uhlig, D., Schuessler, J.A., Bouchez, J., Dixon, J.L., Von Blanckenburg, F., 2017. Quantifying nutrient uptake as driver of rock weathering in forest ecosystems by magnesium stable isotopes. Biogeosciences 14, 3111–3128. https://doi.org/10.5194/bg-14-3111-2017
- Uhlig, D., von Blanckenburg, F., 2019. How Slow Rock Weathering Balances Nutrient Loss During Fast Forest Floor Turnover in Montane, Temperate Forest Ecosystems. Front. Earth Sci. 7, 1–28. https://doi.org/10.3389/feart.2019.00159
- Uhlig, D. (2022): Isotope geochemical dataset on subsoil management experiments at Campus Klein-Altendorf. GFZ Data Services. https://doi.org/10.5880/fidgeo.2022.003
- Vetterlein, D., Kühn, T., Kaiser, K., Jahn, R., 2013. Illite transformation and potassium release upon changes in composition of the rhizophere soil solution. Plant Soil 371, 267–279. https://doi.org/10.1007/s11104-013-1680-6
- Vogl, J., Rosner, M., Kasemann, S.A., Kraft, R., Meixner, A., Noordmann, J., Rabb, S., Rienitz, O., Schuessler, J.A., Tatzel, M., Vocke, R.D., 2020. Intercalibration of Mg Isotope Delta-Scales and Realisation of SI-Traceability for Mg Isotope Amount Ratios and Isotope Delta Values. Geostand. Geoanalytical Res. 1–19. https://doi.org/10.1111/ggr.12327
- Wang, G., Lin, Y., Liang, X., Liu, Y., Xie, L., Yang, Y., Tu, X., 2011. Separation of magnesium from meteorites and terrestrial silicate rocks for high-precision isotopic analysis using multiple collector-inductively coupled plasma-mass spectrometry. J. Anal. At. Spectrom. 26, 1878–1886. https://doi.org/10.1039/c0ja00275e
- Wang, Y., Wu, B., Berns, A.E., Bol, R., Wombacher, F., Ellmer, F., Amelung, W., 2021. A century of

- liming affects the Mg isotopic composition of the soil and crops in a long-term agricultural field at Berlin-Dahlem, Germany. Eur. J. Soil Sci. 72, 300–312. https://doi.org/10.1111/ejss.12951
- Wang, Y., Wu, B., Berns, A.E., Xing, Y., Kuhn, A.J., Amelung, W., 2020. Magnesium isotope fractionation reflects plant response to magnesium deficiency in magnesium uptake and allocation: a greenhouse study with wheat. Plant Soil 455, 93–105. https://doi.org/10.1007/s11104-020-04604-2
- White, A.F., Schulz, M.S., Stonestrom, D.A., Vivit, D. V., Fitzpatrick, J., Bullen, T.D., Maher, K., Blum, A.E., 2009. Chemical weathering of a marine terrace chronosequence, Santa Cruz, California. Part II: Solute profiles, gradients and the comparisons of contemporary and long-term weathering rates. Geochim. Cosmochim. Acta 73, 2769–2803. https://doi.org/10.1016/j.gca.2009.01.029
- Wiegand, B.A., Chadwick, O.A., Vitousek, P.M., Wooden, J.L., 2005. Ca cycling and isotopic fluxes in forested ecosystems in Hawaii. Geophys. Res. Lett. 32, 1–4. https://doi.org/10.1029/2005GL022746
- Wimpenny, J., Colla, C.A., Yin, Q.Z., Rustad, J.R., Casey, W.H., 2014. Investigating the behaviour of Mg isotopes during the formation of clay minerals. Geochim. Cosmochim. Acta 128, 178–194. https://doi.org/10.1016/j.gca.2013.12.012
- Wimpenny, J., Gíslason, S.R., James, R.H., Gannoun, A., Pogge Von Strandmann, P.A.E., Burton, K.W., 2010. The behaviour of Li and Mg isotopes during primary phase dissolution and secondary mineral formation in basalt. Geochim. Cosmochim. Acta 74, 5259–5279. https://doi.org/10.1016/j.gca.2010.06.028
- Wombacher, F., Eisenhauer, A., Böhm, F., Gussone, N., Regenberg, M., Dullo, W.C., Rüggeberg, A., 2011. Magnesium stable isotope fractionation in marine biogenic calcite and aragonite. Geochim. Cosmochim. Acta 75, 5797–5818. https://doi.org/10.1016/j.gca.2011.07.017
- Wombacher, F., Eisenhauer, A., Heuser, A., Weyer, S., 2009. Separation of Mg, Ca and Fe from geological reference materials for stable isotope ratio analyses by MC-ICP-MS and double-spike TIMS. J. Anal. At. Spectrom. 24, 627–636. https://doi.org/10.1039/b820154d
- Wrobel, Katarzyna, Karasinski, J., Tupys, A., Negrete, M.A.A., Halicz, L., Wrobel, Kazimierz, Bulska, E., 2020. Magnesium Isotope Fractionation in Chlorophyll-a Extracted from Two Plants with Different Pathways of. Molecules 25, 1–12. https://doi.org/doi:10.3390/molecules25071644
- Young, E.D., Galy, A., 2004. The Isotope Geochemistry and Cosmochemistry of Magnesium, in: Reviews in Mineralogy and Geochemistry. pp. 197–230. https://doi.org/10.2138/gsrmg.55.1.197

#### 12. Figures

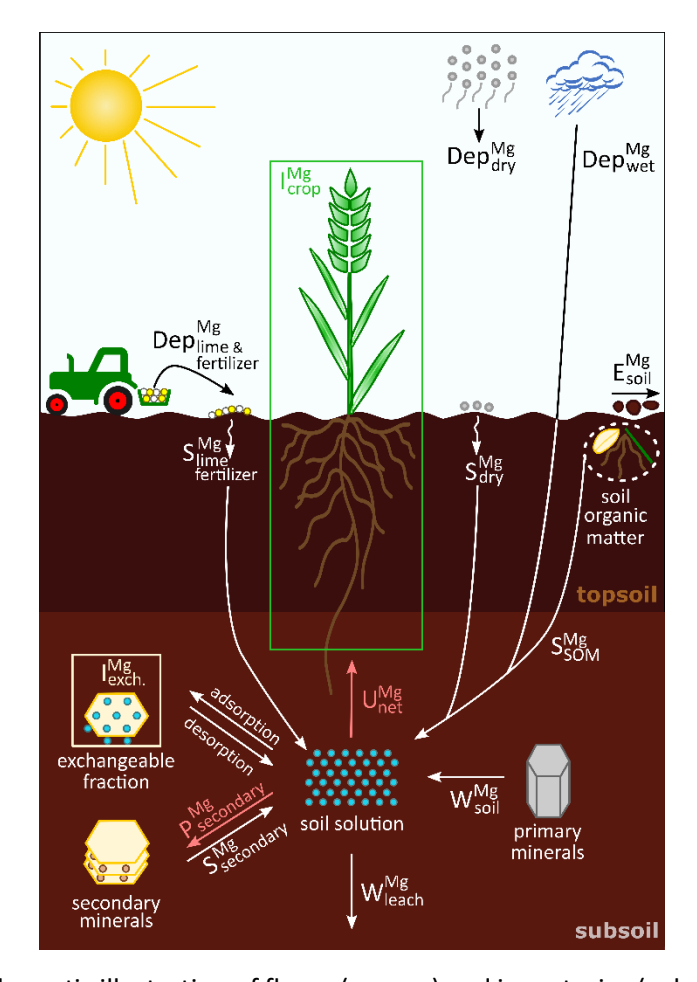


**Figure 1** Simplified schematic illustration of fluxes (arrows) and inventories (coloured frames, "I") in an agricultural soil-plant system. Colour coding of text and arrows: Black (aboveground fluxes) and white (belowground fluxes) formatting indicate processes taking place without fractionation of Mg isotopes, and red formatting indicates processes taking place with fractionation of Mg isotopes. Magnesium fluxes indicate deposition ("Dep") of agricultural inputs such as fertilizer and agricultural lime, and atmospheric inputs (wet and dry); erosion ("E"); precipitation ("P") of secondary solids; solubilisation ("S") of solids; crop uptake ("U"); chemical weathering and leaching ("W"). Detailed information on the metrics is provided in Table 1. Figure is not drawn to scale, e.g., arrow size is independent of the magnitude of a given flux.

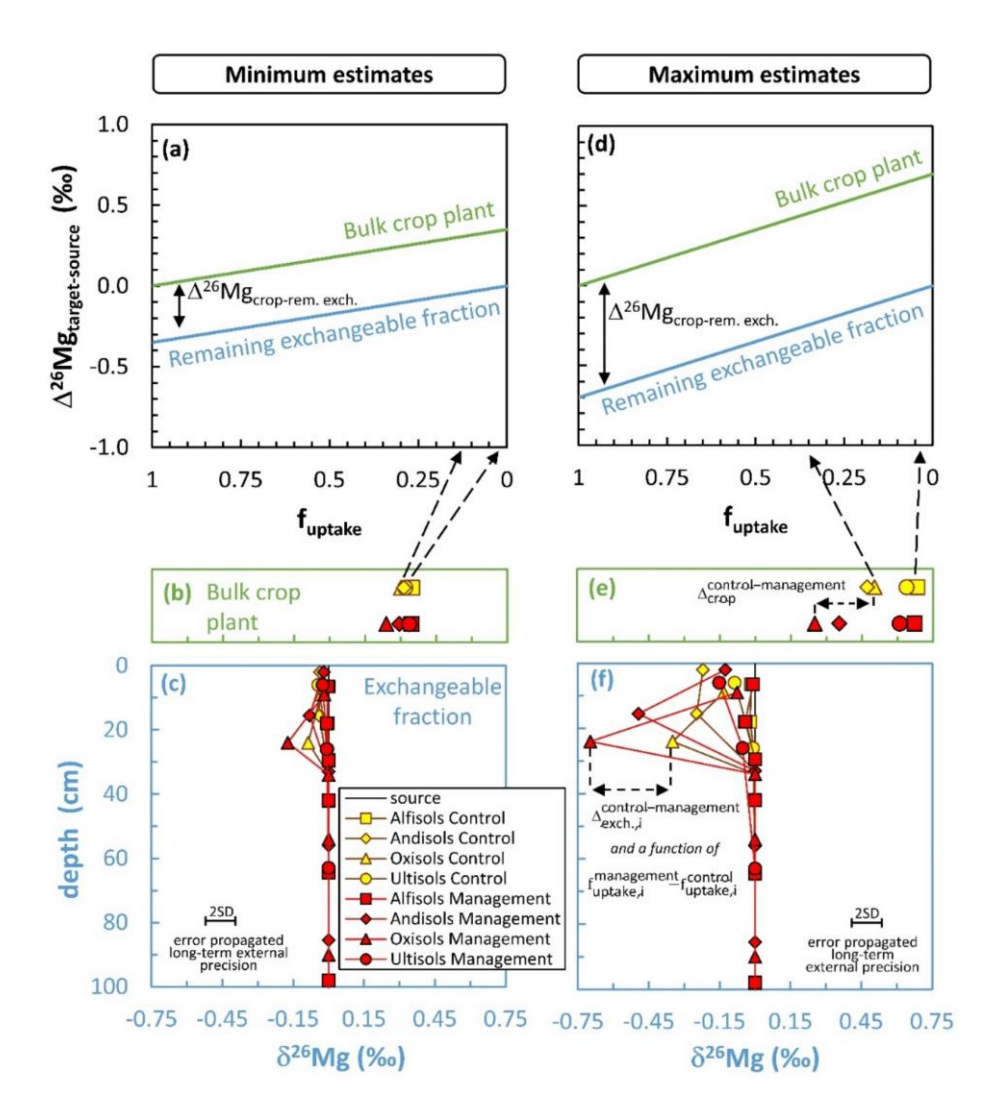
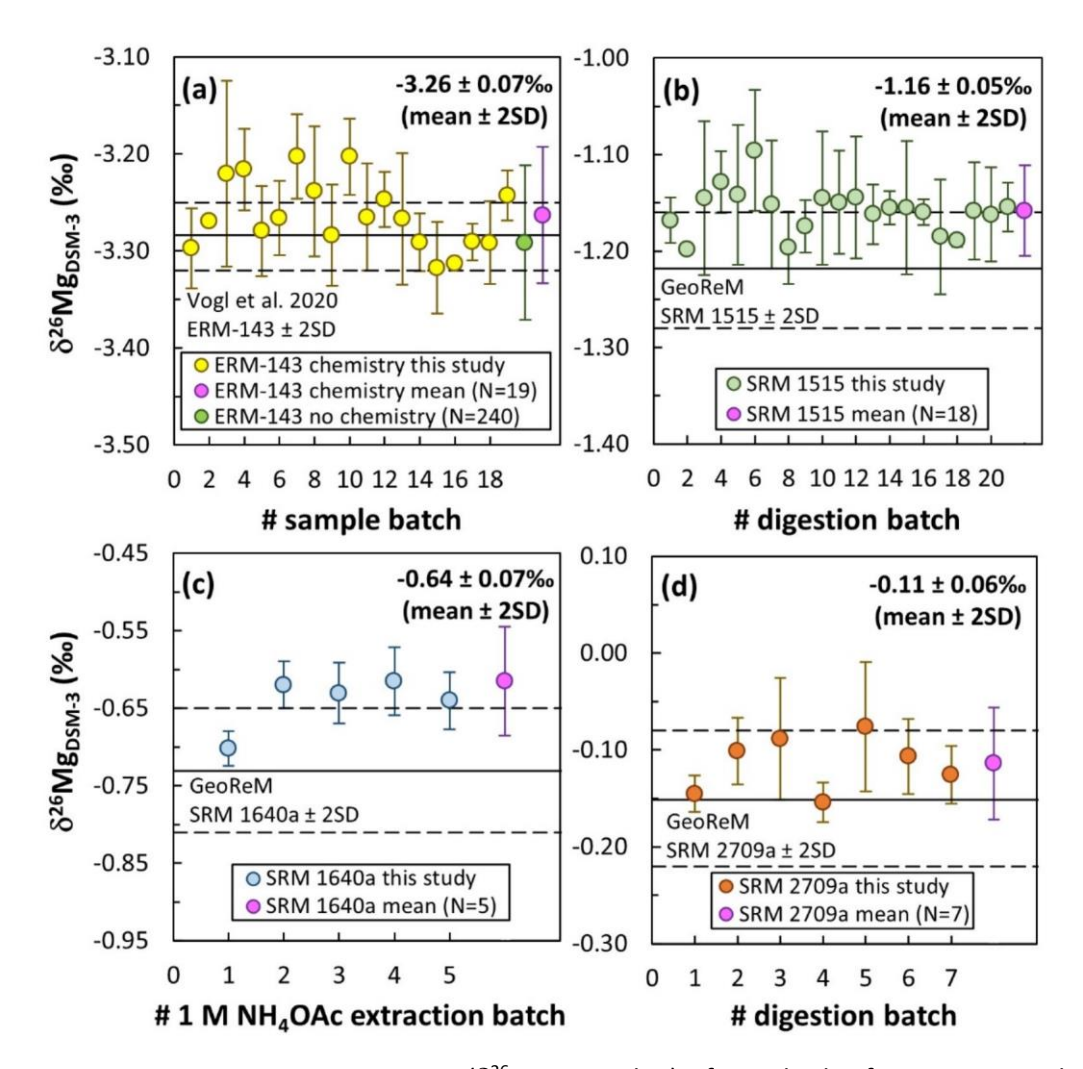
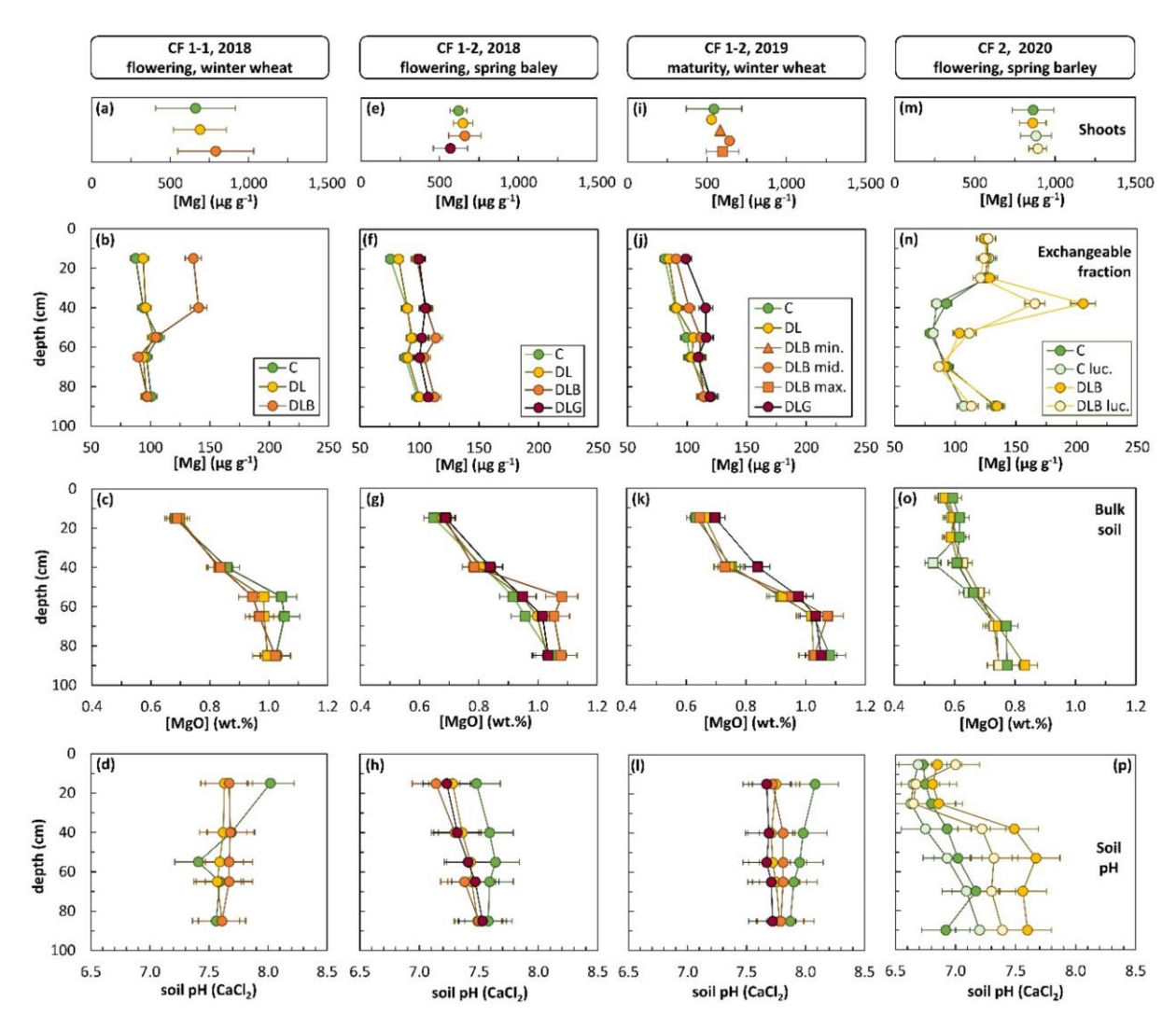


Figure 2 Conceptual graphical representation of the partitioning of Mg isotopes in the soil-plant system. Upper panels (a) and (d) show the difference in the Mg isotope composition ( $\delta^{26}$ Mg value) of the target and source compartments ( $\Delta^{26}$ Mg<sub>target-source</sub>) as a function of the relative proportion of Mg taken up by crops to the Mg supplied to crops (f<sub>uptake</sub>). The source compartment is represented by the initial exchangeable fraction that is the exchangeable fraction before Mg uptake by crops, and the target compartments comprise bulk crop plant and the remaining exchangeable fraction after Mg uptake by crops. Lower panels (b)-(c) and (e)-(f) illustrate the Mg isotope composition of bulk crops and the exchangeable fraction of soil at individual soil horizons without (control) and with simulated subsoil management (management). Minimum and maximum estimates on the plant uptake-related apparent Mg isotope fractionation factor ( $\Delta^{26}$ Mg<sub>plant-source</sub>), Mg inventory in crops at maturity stage  $(I_{crop,t_m}^{Mg})$ , and soil horizon specific proportions of Mg uptake  $(f_{root,i})$  are provided in section 3.3.3 and in Supplementary Information 2 and 3. Soils according to the USDA Soil Taxonomy (Soil Survey Staff, 1999) were selected to represent low, medium and high inventories of exchangeable Mg. For ease of display Gelisols, Mollisols and Vertisols were not shown as  $\delta^{26} Mg_{crop}$  values and the depth distribution of  $\delta^{26}$ Mg<sub>rem.exch.</sub> values overlap with Alfisols. Sloped arrows illustrate  $f_{uptake}$  at minimum and maximum estimates. Horizontal arrows indicate i) Mg isotope shifts in crops and the exchangeable fraction of Mg in soil among the control and management ( $\Delta_{crop}^{control-management}$ ,  $\Delta_{exch,i}^{control-management}$ ), and ii) the isotope-derived difference in the Mg use efficiency among management and the control  $-\,f_{uptake,i}^{control})$ . The long-term external precision at the two-fold standard deviation (2SD) level is compiled from Mg isotope studies from 2019-2021 (compiled and error propagated in Supplementary Information 4).



**Figure 3** Magnesium isotope composition ( $\delta^{26}$ Mg<sub>DSM-3</sub> value) of standard reference materials (SRM) used to determine the accuracy and precision of the analytical method over the course of 36 months. Panel (a) shows accuracy and precision of the cation-exchange chromatography method as ERM-AE143 was processed as sample with each sample batch yielding a long-term external precision of 0.07% (2SD). Panels (b) – (d) illustrate the accuracy and precision of microwave assisted sample digestions or the exchangeable fraction of Mg in soil. Specifically, panel (b) displays accuracy and precision of NIST SRM 1515 apple leaves representing plant samples, panel (c) shows accuracy and precision of NIST SRM 1640a natural water representing the exchangeable fraction of Mg in soil (1M NH<sub>4</sub>OAc extraction), panel (d) shows accuracy and precision of NIST SRM 2709a San Joaquin soil representing bulk soil samples. Solid and dashed lines denote mean values and the two-fold standard deviation (2SD) on  $\delta^{26}$ Mg published in previous studies and except for ERM-AE143 (Vogl et al., 2020) compiled in the GeoReM database (Jochum et al., (2005), http://georem.mpch-mainz.gwdg.de). Error bars denote to the 2SD of repeated analyses measured in one analytical session, and 2SD on the mean values of the entirety of sample or digestion batches.



**Figure 4** Magnesium concentrations of shoots, the exchangeable fraction of Mg in soil (1M  $NH_4OAc$  extraction), bulk soil, and soil pH (0.01M  $CaCl_2$ ) at the central field trials CF 1-1, CF 1-2 and CF 2 cultivated with winter wheat (panels (a)-(d) and (i)-(l)) and spring barley (panels (e)-(h) and (m)-(p)) under varying subsoil managements and the control. Error bars of pooled soil samples (bulk soil and the exchangeable fraction) denote a relative uncertainty of 5%, error bars of shoots denote the standard error of field replicates, and error bars of soil pH denote the two-fold standard error (2SE) of repeat analyses of NIST SRM 2709a. C: control; C luc.: control + lucerne; DL: deep loosening; DLB: deep loosening + biowaste compost; DLG: deep loosening + green waste compost; DLB luc.: deep loosening + biowaste compost + lucerne.

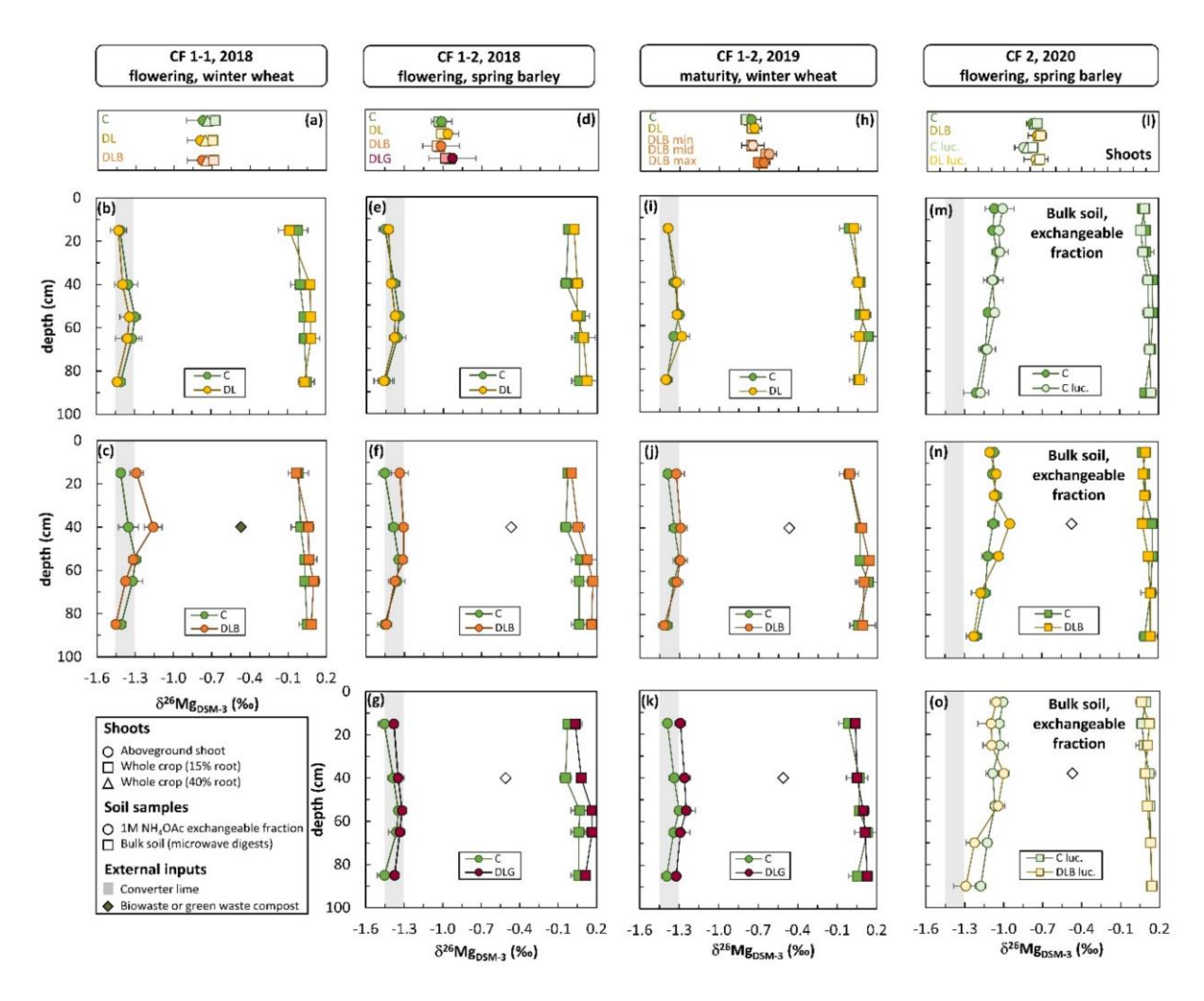
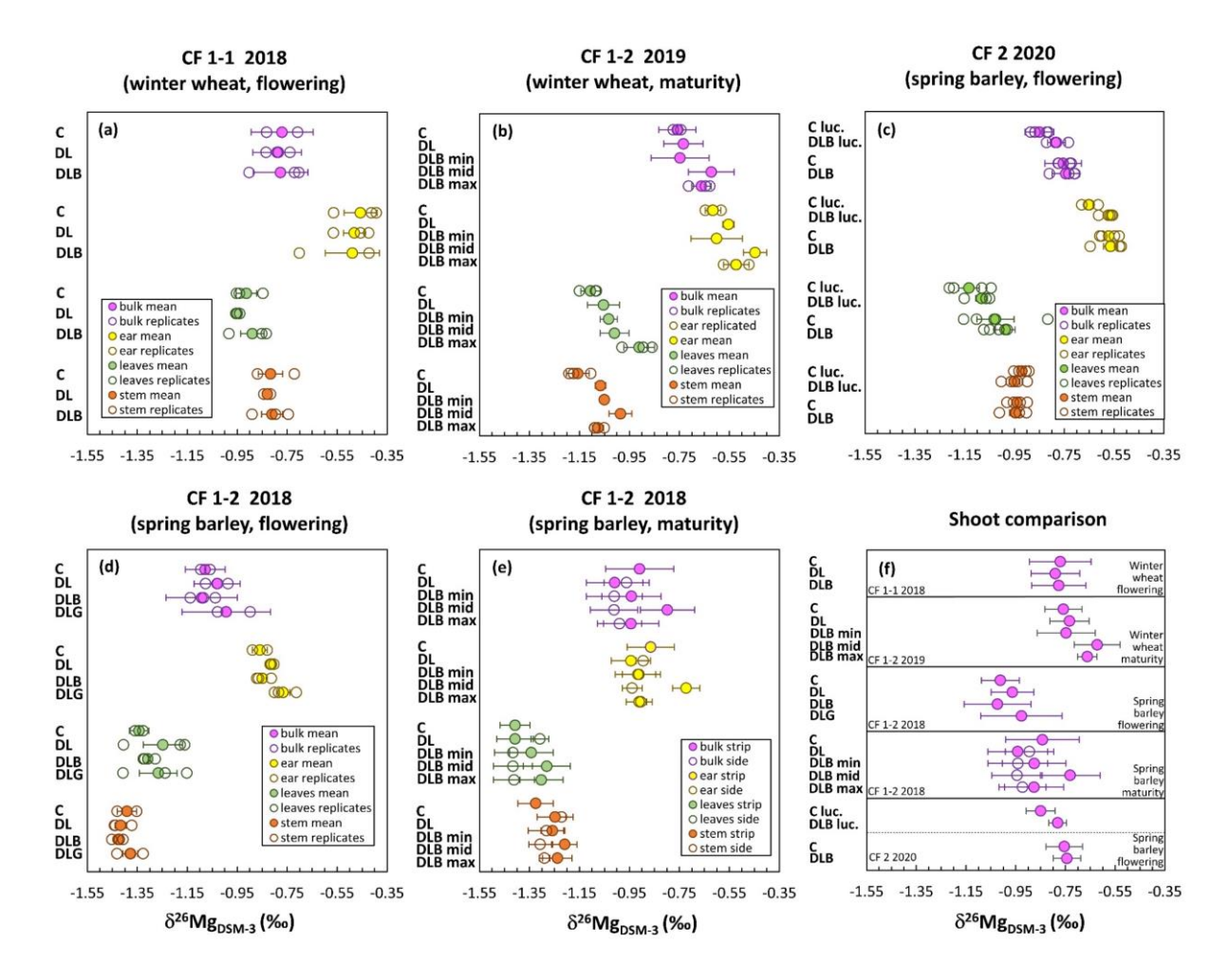
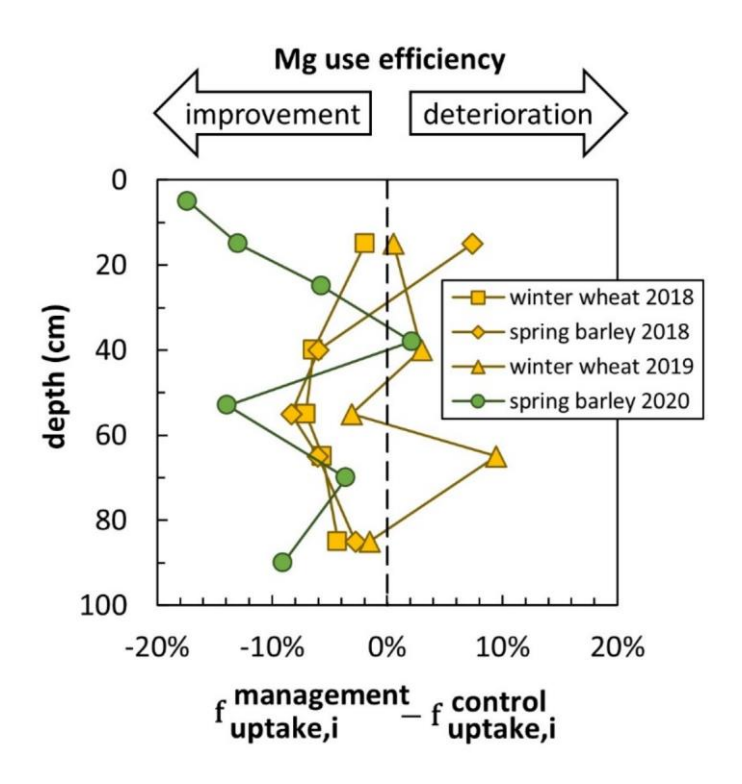


Figure 5 Magnesium isotope composition ( $\delta^{26}$ Mg<sub>DSM-3</sub> value) of shoots, the exchangeable fraction of Mg in soil (1M NH<sub>4</sub>OAc extraction) and bulk soil at the central field trials CF 1-1, CF 1-2 and CF 2 cultivated with winter wheat (panels (a)-(c) and (h)-(k)) and spring barley (panels (d)-(g) and (l)-(o)) under varying subsoil managements and the control. As crop roots were not sampled in this study (section 4.3) the bulk whole crop Mg isotope composition was estimated by using literature data on  $\Delta^{26}$ Mg<sub>root-stem</sub>, two scenarios on the relative contribution of root biomass on whole crop biomass (15% and 40%) and the Mg concentration of roots (section 4.5.1). For ease of display,  $\delta^{26}$ Mg values of converter lime (grey bar displays the internal precision of the  $\delta^{26} Mg_{lime}$  value) and biowaste and green waste compost (plotted at depth of incorporation; white fill denotes informative values only as reference samples of compost applied to CF 1-2 and CF 2 were unavailable for analyses) are illustrated with soil compartments. Error bars of pooled soil samples (bulk soil and the exchangeable fraction) denote the two-fold standard deviation (2SD) of repeat analyses in the same analytical session and error bars of crop samples denote the error propagated standard error of biomass, Mg concentrations and  $\delta^{26}$ Mg values of the individual crop organs from all field replicates. For ease of display error bars of crop samples are only shown for bulk shoots. Note: In panel (c) soil depth profiles for deep loosening and compost (min, max) are not available. Conversely, soil depth profiles are available for the subsoil management deep loosening and green waste. C: control; C luc.: control + lucerne; DL: deep loosening; DLB: deep loosening + biowaste compost; DLG: deep loosening + green waste compost; DLB luc.: deep loosening + biowaste compost + lucerne.



**Figure 6** Magnesium isotope composition ( $\delta^{26}$ Mg<sub>DSM-3</sub> value) of crops at the central field trials CF 1-1, CF 1-2 and CF 2 cultivated with winter wheat and spring barley under varying subsoil managements and the control. Panel (a) – (e) show the Mg isotope composition of the plant organs ear, leaf, and stem along with  $\delta^{26}$ Mg values of bulk shoots. Panel (f) provides a comparison of the average  $\delta^{26}$ Mg value of shoots from field replicates shown in panels (a) – (e). Apart from panel (e) and (d) open symbols refer to field replicates and filled symbols indicate the average value of the field replicates. In panel (e) and (d) filled symbols refer to samples collected on the melioration strip (denoted strip) and open symbols refer to samples collected next to the melioration strip (denoted side). C: control; C luc.: control + lucerne; DL: deep loosening; DLB: deep loosening + biowaste compost; DLG: deep loosening + green waste compost; DLB luc.: deep loosening + biowaste compost + lucerne.



**Figure 7** Graphical visualisation of the depth distribution on differences in the isotope-derived Mg use efficiency among management and the control ( $f_{uptake,i}^{management} - f_{uptake,i}^{control}$ , equation 12, section 3.3.2). Management refers to deep loosening at CF 1-1 and CF 1-2 (yellow colour) and using lucerne as deeprooting pre-crop at CF 2 (green colour).

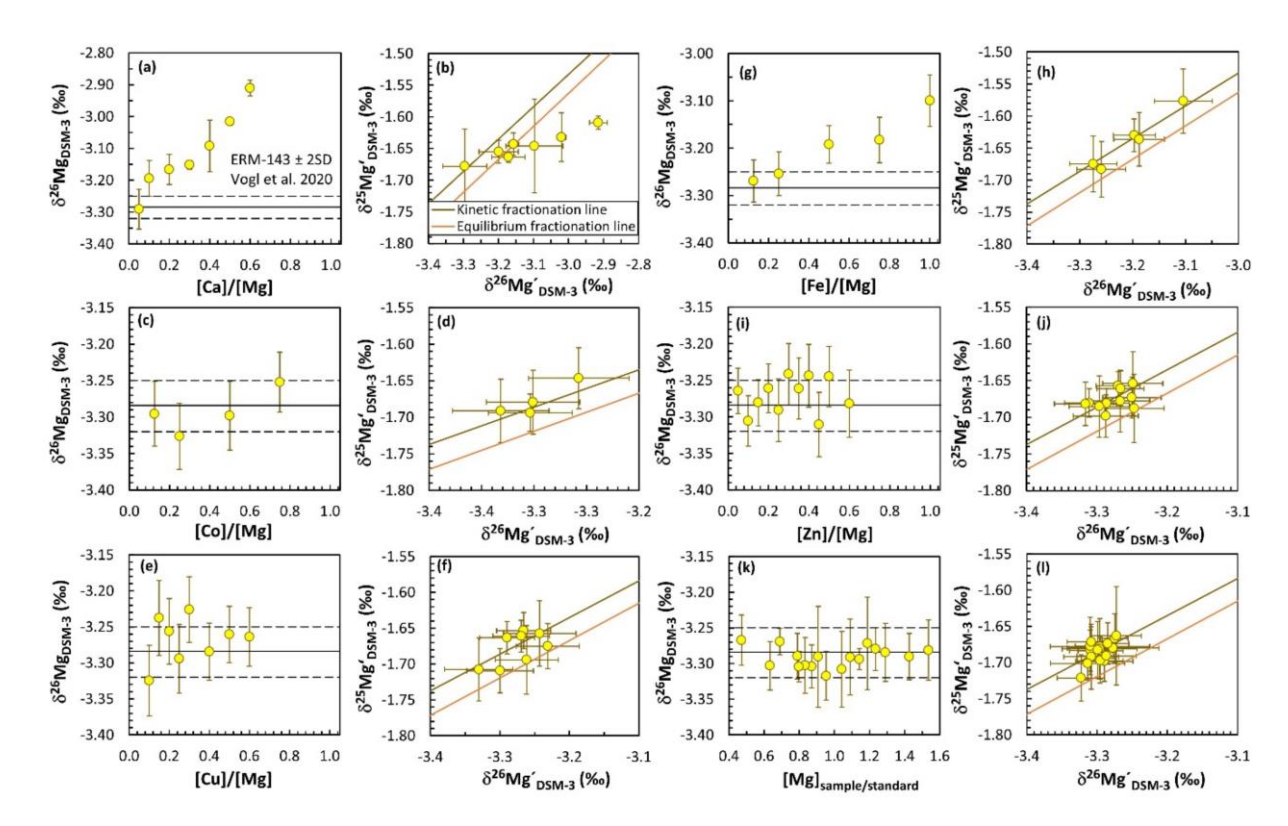


Figure A1 Determination of effects on sample impurities of Ca (panel (a) and (b), Co (panel (c) and (d)), Cu (panel (e) and (f)), Fe (panel (g) and (h)), Zn (panel (i) and (j)), and concentration mismatch (panel ((k) and (l)) during MC-ICP-MS analyses. Accuracy and precision are shown in left-hand panels and deviations from the equilibrium and kinetic isotope fractionation lines in the three-isotope plot are shown in right-hand panels. Linearized delta values ( $\delta^{26}$ Mg′ and  $\delta^{25}$ Mg′) were calculated following Young and Galy (2004). Solid and dashed lines refer to the  $\delta^{26}$ Mg value ± two-fold standard deviation (2SD) of the bracketing standard ERM-AE43 on the DSM-3 scale obtained from an inter-laboratory comparison (Vogl et al., 2020). Error bars denote the internal precision except for Ca impurity and concentration mismatch experiments shown in panel (a) and (k) in which the error bar denotes the two-fold standard deviation (2SD) of two sample replicates measured in one analytical session. The Mg concentration was kept at 600 ng g<sup>-1</sup> for all doping experiments. Results of the concentration mismatch experiments were not discussed in this Appendix, but are in agreement with findings from An et al., (2014), Teng and Yang (2014), and Hu and (Teng 2019).

## 13. Tables

14. <b>Table 1</b> Gloss	ary of metrics					
Magnesium fluxes (	(e.g., in mg m <sup>-2</sup> γr <sup>-1</sup> )					
$Dep^{Mg}_{wet}$	Wet atmospheric deposition flux of Mg, section 3.2, Figure 1					
$Dep^{Mg}_{dry}$	Dry atmospheric deposition flux of Mg, section 3.2, Figure 1					
Dep <sup>Mg</sup> <sub>fertilizer</sub>	Fertilizer application flux of Mg, section3.2, Figure 1					
$Dep^{Mg}_{lime}$	Agricultural lime application flux of Mg, section 3.2, Figure 1					
S <sup>Mg</sup> dry	Dry atmospheric solubilisation flux of Mg, section 3.2, Figure 1					
S <sup>Mg</sup> Sfertilizer	Fertilizer solubilisation flux of Mg, section3.2, Figure 1					
S <sup>Mg</sup> <sub>lime</sub>	Agricultural lime flux of Mg, section 3.2, Figure 1					
S <sub>SOM</sub>	Soil organic matter solubilisation flux of Mg, section 3.2, Figure 1					
S <sup>Mg</sup> secondary	Secondary solid solubilisation flux of Mg, section 3.2, Figure 1					
P <sub>secondary</sub>	Net neoformation of secondary solids flux of Mg, section 3.2, Figure 1					
$W_{ m soil}^{ m Mg}$	Chemical weathering flux of Mg, section 3.2, Figure 1					
E <sub>soil</sub>	Soil erosion flux of Mg, section 3.2, Figure 1					
W <sub>leach</sub>	Leaching loss flux of Mg into groundwater aquifers, section 3.2, Figure 1					
$U_{ m net}^{ m Mg}$	Net crop uptake flux of Mg, section 3.2, Figure 1					
Magnesium invento	ories/ stocks/ pools (e.g., in g m <sup>-2</sup> )					
I <sup>Mg</sup> crop or organ	Inventory of Mg either in bulk crop or of individual crop organs, section 3.1, 3.3.3, equation 1, equation 4, equation 8, equation 13					
$I_{soil}^{Mg}$	Inventory of Mg in bulk soil, section 6.3					
I <sup>Mg</sup> initial exch.	Inventory of Mg in the exchangeable soil fraction as integral over all soil horizons, section 3.1, 3.3, equation 2, equation 4					
I <sup>Mg</sup> rem. exch.,i	Soil horizon specific inventory of Mg in the exchangeable fraction, section 3.3.1, equation 8					
Mass fractions (dim	nensionless)					
$f_{\text{root,i}}$	Fraction of root biomass in soil horizon i to total root biomass, section 3.3.1, equation 8, equation 9					
forgan	Fraction of the biomass of an organ to the total biomass, section 4.5.1, equation 14, equation 15					

$f_{root,i}$	9
$f_{organ}$	Fraction of the biomass of an organ to the total biomass, section 4.5.1, equation 14, equation 15
$f_{uptake}^{Mg}$	Fraction of Mg taken up by crops relative to Mg available in the exchangeable fraction, 3.3, equation 4, equation 5, equation 6, equation 7, Figure 2
$f_{uptake,i}^{Mg}$	Fraction of Mg taken up by crops from soil horizon i to Mg available in the exchangeable fraction of soil horizon i, section 3.3.1, equation 8, (equation 5, equation 6, equation 7)
$f_{uptake,i}^{management} - f_{uptake,i}^{control} \\$	Difference in the isotope-derived Mg use efficiency among management and control, section 3.3.2, equation 12, Figure 2

### Magnesium isotopes (in ‰, or dimensionless\*)

$\delta^{26} Mg_{compartment}$	Normalised $^{26}$ Mg/ $^{24}$ Mg isotope ratio in compartments (e.g., soil, crop) relative to DSM-3, section 3.3, 4.5.1, equation 3, equation 5, equation 6, equation 7, equation 9, equation 10, equation 11, equation 12, equation 15
$\alpha^{26} Mg_{crop\text{-}rem.exch.}{}^*$	Plant uptake-related Mg isotope fractionation factor between crop and the exchangeable fraction, section 3.3, equation 3
$\Delta^{26} Mg_{crop\text{-}rem.exch.}$	Isotope difference between crop and the exchangeable fraction, section 3.3, equation 3, equation 6, equation 7, equation 12, Figure 2
$\Delta_{exch.,i}^{control-management}$	Isotope difference of the exchangeable fraction among the control and subsoil managed trial, section 3.3.2, equation 11, Figure 2
$\Delta_{crop}^{control-management}$	Isotope difference of crop among the control and subsoil managed trial, section 3.3.2, equation 10

**Table 2** Magnesium concentration and Mg isotope composition of bulk crop samples averaged from individual field replicates at central field trials.

ITOTT IIIdividual fie	whole crop	whole crop			whole crop		whole crop	
Treatment	(15% root) <b>Mg</b>			(15% root*) $\delta^{26}$ Mg <sub>DSM-3</sub> SE		(40% root*) 8 <sup>26</sup> Mgpoure SF		
	μg g <sup>-1</sup> )	(%)	(‰)	(‰)	(‰)	(%)	(‰)	
CF 1 1 (winter wh		, ,	(700)	(700)	(700)	(700)	(700)	
CF 1-1 (winter who		ng 2018)						
C (mean) C (SE)	672 73	-0.77	0.13	-0.73	0.12	-0.68	0.11	
DL (mean) DL (SE)	697 79	-0.79	0.11	-0.75	0.10	-0.69	0.10	
DLB (mean) DLB (SE)	782 87	-0.78	0.12	-0.74	0.11	-0.69	0.10	
CF 1-2 (spring bar	ley at flowerir	ng 2018)						
C (mean) C (SE)	637 46	-1.01	0.08	-1.02	0.10	-1.03	0.15	
DL (mean) DL (SE)	661 49	-0.96	0.08	-0.98	0.10	-1.01	0.16	
DLB (mean) DLB (SE)	667 70	-1.02	0.14	-1.03	0.14	-1.05	0.17	
DLG (mean) DLG (SE)	593 75	-0.93	0.18	-0.95	0.17	-0.98	0.18	
CF 1-2 (spring bar	ley at maturit	y stage 2018)						
С	683	-0.84	0.12	-0.85	0.11	-0.87	0.10	
DL (strip)	743	-0.94	0.11	-0.94	0.10	-0.94	0.09	
DL (side)	719	-0.89	0.08	-0.89	0.08	-0.89	0.07	
DLB low (strip) DLB low (side)	695 689	-0.88 -0.94	0.11 0.11	-0.88 -0.94	0.10 0.10		0.09 0.09	
DLB mid. (strip) DLB mid. (side)	785 758	-0.73 -0.94	0.08 0.09	-0.74 -0.95	0.08 0.08		0.07 0.08	
DLB max. (strip) DLB max. (side)	762 708	-0.88 -0.92	0.10 0.08	-0.88 -0.92	0.09 0.08		0.08 0.07	
CF 1-2 (winter who	eat at maturit	y stage 2019)						
C (mean) C (SE)	517 49	-0.76	0.07	-0.77	0.09	-0.80	0.11	
DL	504	-0.73	0.05	-0.74	0.05	-0.75	0.05	
DLB min.	551 601	-0.75	0.09 0.06	-0.75	0.08	-0.76 -0.65	0.07	
DLB mid.  DLB max. (mean)	601 563	-0.62 -0.66	0.06	-0.63 -0.68	0.05		0.05	
DLB max. (SE)	29							
CF 2 (spring barley	at flowering	2020)						
C luc. (mean) C luc. (SE)	859 53	-0.85	0.07	-0.82	0.07	-0.78	0.09	
C (mean) C (SE)	844 65	-0.75	0.09	-0.74	0.09	-0.72	0.10	
DLB luc. (mean) DLB luc. (SE)	863 57	-0.78	0.05	-0.77	0.05	-0.75	0.09	
DLB (mean) DLB (SE)	832 73	-0.74	0.07	-0.73	0.07	-0.72	0.09	

<sup>\*</sup> Bulk whole crop at flowering was calculated for two root scenarios (min, max estimation) using literature data on  $\Delta_{\text{root-stem}}$  and the Mg concentration in roots (see section 4.5.1). Note: To consider root mortality at maturity stage only half of the root biomass used to estimate whole bulk crop at flowering stage was used to estimate the  $\delta^{26}\text{Mg}$  value of whole bulk crop sampled at maturity stage.

SE denotes to the standard error, which was estimated by gaussian error propagation of the standard errors obtained from field replicates from i) the Mg concentration, ii) the biomass and iii) in case of the  $\delta^{26} Mg_{shoot\ or\ whole\ crop}$  value from the  $\delta^{26} Mg\ value\ of\ individual\ crop\ organs.$